SPECKLE-NOISE REDUCTION IN KNEE ARTICULAR CARTILAGE ULTRASOUND IMAGE USING ANISOTROPIC DIFFUSION

MUHAMMAD SHOAIB ALI

FACULTY OF ENGINEERING
UNIVERSITY OF MALAYA
KUALA LUMPUR

2020

SPECKLE-NOISE REDUCTION IN KNEE ARTICULAR CARTILAGE ULTRASOUND IMAGE USING ANISOTROPIC DIFFUSION

MUHAMMAD SHOAIB ALI

DISSERTATION SUBMITTED IN FULFILMENT OF THE REQUIREMENTS FOR THE DEGREE OF MASTER OF ENGINEERING SCIENCE

FACULTY OF ENGINEERING
UNIVERSITY OF MALAYA
KUALA LUMPUR

2020

UNIVERSITY OF MALAYA

ORIGINAL LITERARY WORK DECLARATION

Name of Candidate: **Muhammad Shoaib Ali**

Matric No: **KGA180003**

Name of Degree: **Master of Engineering Science (Electrical)**

Title of Project Paper/Research Report/Dissertation/Thesis ("this Work"):

SPECKLE-NOISE REDUCTION IN KNEE ARTICULAR CARTILAGE ULTRASOUND IMAGE USING ANISOTROPIC DIFFUSION

Field of Study: **Signal and Systems**

I do solemnly and sincerely declare that:

(1) I am the sole author/writer of this Work;
(2) This Work is original;
(3) Any use of any work in which copyright exists was done by way of fair dealing and for permitted purposes and any excerpt or extract from, or reference to or reproduction of any copyright work has been disclosed expressly and sufficiently and the title of the Work and its authorship have been acknowledged in this Work;
(4) I do not have any actual knowledge nor do I ought reasonably to know that the making of this work constitutes an infringement of any copyright work;
(5) I hereby assign all and every rights in the copyright to this Work to the University of Malaya ("UM"), who henceforth shall be owner of the copyright in this Work and that any reproduction or use in any form or by any means whatsoever is prohibited without the written consent of UM having been first had and obtained;
(6) I am fully aware that if in the course of making this Work I have infringed any copyright whether intentionally or otherwise, I may be subject to legal action or any other action as may be determined by UM.

Candidate's Signature Date:

Subscribed and solemnly declared before,

Witness's Signature Date:

Name:

Designation:

SPECKLE-NOISE REDUCTION IN KNEE ARTICULAR CARTILAGE ULTRASOUND IMAGE USING ANISOTROPIC DIFFUSION

ABSTRACT

Knee arthritis is the most common type of arthritis which effects the people and may cause severe pain to the patient and can lead to joint effusion. Ultrasound (US) imaging is an appropriate and consistent substitute for other imaging techniques like magnetic resonance imaging or X-rays in the investigation or screening of knee injury. Nevertheless, one of the major problems in US images which make the analysis of these images hard is the presence of speckle noise. For the reduction of speckle noise, the performance of the anisotropic method is found much better over other approaches. In removing the speckle noise, mostly used methods diffuse the edges during the diffusion of the homogenous region of US images. Therefore, the very critical task is to preserve the edges during the diffusion process. In this research, a method based on Anisotropic Diffusion (AD) is proposed to reduce the speckle noise. The proposed variation in the AD method not only reduces the speckle noise but also preserves the edges and other important detail of images efficiently. Four gradient thresholds are proposed instead of one to have comprehensive information of all neighbouring pixels. A new diffusivity function is also proposed to preserve the edges by stopping diffusion abruptly nears edges. Four different evaluation metrics i.e. Peak Signal-to-Noise Ratio (PSNR), Structure Similarity Index Measurement (SSIM), Figure of Merit (FOM), and Equivalent Number of Looks (ENL) are used to evaluate the performance of the proposed method. Numerical results attained by simulations show that the proposed method reduces the speckle noise very effectively and preserves the edges as well.

Keywords: Anisotropic Diffusion, Diffusivity function, Edge preservation, Speckle noise

PENGURANGAN KEBISIGAN BINTIK DALAM IMEJ ULTRABUNYI RAWAN ARTIKULAR LUTUT MENGGUNAKAN PENYEBARAN ANISOTROPIK

ABSTRAK

Arthritis lutut adalah jenis arthritis yang paling biasa yang memberi kesan kepada orang-orang dan boleh menyebabkan kesakitan yang teruk kepada pesakit dan boleh menyebabkan pengaliran bersama. Pengimejan ultrabunyi (US) adalah pengganti yang sesuai dan konsisten bagi teknik-teknik pengimejan lain seperti pengimejan resonans magnetik atau sinar-X dalam penyiasatan atau penyaringan kecederaan lutut. Walau bagaimanapun, terdapat dua masalah utama dalam imej US yang menjadikan analisis imej-imej ini susah iaitu nisbah perbandingan rendah dan kehadiran hingar bintik. Untuk mengurangkan hingar bintik, prestasi kaedah anisotropik didapati jauh lebih baik berbanding pendekatan lain. Dalam mengasingkan kebisingan bintk, kebanyakan kaedah yang digunakan meresap pinggir semasa penyebaran wilayah homogen imej AS. Oleh itu, tugas yang sangat penting adalah untuk mengekalkan pinggir semasa proses penyebaran. Dalam penyelidikan ini, satu kaedah berdasarkan penyebaran anisotropik (AD) dicadangkan untuk mengurangkan hingar bintik. Variasi yang dicadangkan dalam kaedah AD bukan sahaja mengurangkan kebisingan tetapi juga memelihara pinggir dan maklumat penting lain dalam imej dengan efisien. Empat ambang kecerunan dicadangkan dan bukannya satu untuk mengandungi maklumat yang komprehensif mengenai semua piksel sebelah. Fungsi diffusivity baru juga dicadangkan supaya mengekalkan pinggir dengan menghentikan penyebaran tiba-tiba berhampiran pinggir. Empat tahap ujian metrik yang berbeza iaitu Nisbah Isyarat Dengan Hingar Puncak (PSNR), Pengukuran Indeks Persamaan Struktur (SSIM), Rajah Merit (FOM), dan Jumlah Kesamaan Setara (ENL) digunakan untuk menilai prestasi kaedah yang dicadangkan. Keputusan berangka yang dicapai oleh simulasi menunjukkan bahawa kaedah yang dicadangkan dapat mengurangkan hingar bintik dengan berkesan sementara mengekalkan pinggir.

Keywords: Penyebaran anisotropik, Fungsi penyebaran, Pemeliharaan pinggir , Hingar bintik

ACKNOWLEDGEMENTS

First, I would like to thank almighty Allah for giving me the health and strength to complete my studies.

I would like to express my deep respect and heartiest appreciation to both supervisors Dr. Chuah Joon Huang and Dr. Lai Khin Wee for their guidance and support at every step. Their devoted help and welcoming hands were always there for me in every situation. In addition, I am also grateful to HEC Pakistan for providing financial support.

I would also very thankful and grateful to my mother for her endless love and prayers which always keep me high. This work was not possible for me without the support and backing of my brothers, sister and other family members. I am also very obliged to my wife for her unfailing support and patience during my studies. Without her understanding, I would not be able to achieve my goals.

Muhammad Shoaib Ali

TABLE OF CONTENTS

LIST OF FIGURES

LIST OF TABLES

LIST OF SYMBOLS AND ABBREVIATIONS

AD	:	Anisotropic Diffusion
AWMF	:	Adaptive Weighted Median Filter
CNN	:	Convolutional Neural Network
CT	:	Computed Tomography
DPAD	:	Detail Preserving Anisotropic Diffusion
ENL	:	Equivalent Number of Looks
FOM	:	Figure of Merit
G (σ)	:	Gaussian Filter
K	:	Gradient Threshold
LPND	:	Laplacian Pyramid Nonlinear Diffusion
MAD	:	Median Absolute Deviation
MAE	:	Mean Absolute Error
MSE	:	Mean Square Error
MRI	:	Magnetic Resonance Imaging
NE	:	North-East
NEWS	:	North-East and West-South
NCD	:	Nonlinear Complex Diffusion
OSRAD	:	Oriented Speckle Reducing Anisotropic Diffusion
PDE	:	Partial Differential Equations
PM	:	Perona-Malik
PSNR	:	Peak Signal to Nosie Ratio
SAR	:	Synthetic Aperture Radar
SE	:	South-East
SRAD	:	Speckle Reducing Anisotropic Diffusion

SSIM	:	Similarity Index Measure
US	:	Ultrasound
WN	:	West-North
WNSE	:	West-North and South-East
WS	:	West-South
∇I	:	Gradient of Image
c(.)	:	diffusivity function
$\Psi(x)$	:	Flow function

CHAPTER 1: INTRODUCTION

1.1 Background

Knee pain is a common complaint that affects people of all ages. The pain in knee joints is prominent in elderly people but young and children also suffer from this. There could be different reasons for the knee pain as joints in the knee are made up of bones, ligaments, cartilage and fluids. The pain may cause due to some injury, broken ligament or also due to torn cartilage. One of the most common problems in the knee is arthritis. Different arthritis is rheumatoid Arthritis, posttraumatic Arthritis and osteoarthritis. These knee injuries can also lead to disability and according to one survey, these will be the fourth-largest cause of disability in the world by 2020 (Gohal et al., 2018).

To visualize these knee injuries and arthritis, different medical imaging systems are used. X-rays, Magnetic Resonance Imaging (MRI), Computed Tomography (CT), and Ultrasound (US) are typically used for the examination (Hossain et al., 2014). Among these, MRI is very expensive and not suitable for implanted patients. While CT not only releases a high level of radiation but also has a constraint for detecting a fracture, meanwhile X-ray produces ionizing radiation and also lacks in the description of soft tissues (Faisal et al., 2015). Unquestionably, all the mentioned medical imaging methods have some drawbacks.

Consequently, US imaging is considered as a valuable and useful approach for knee arthritis assessment, especially in terms of cost, safety, and ease of use. Despite having a lot of advantages, US images suffer from two main drawbacks, namely the presence of speckle noise, and having a low contrast ratio. Hossain et al. (2014) enhance the contrast of the US image and propose a method to detect the cartilage shape of the knee joint more accurately. The second main problem with the US image is speckles noise. The speckle noise is multiplicative noise and inherent property in US images (Tur, Chin, & Goodman, 1982). Its presence is due to the superposition of acoustic echo and generates a complicated interference pattern. This pattern is produced due to interferes with the US with the object of comparable size to sound wavelength. This speckle-noise disguises the relevant information of the patient in the image. Hence, it is very important to retain the important detail of the original image by lowering the effect of speckle noise.

Among the different methods, the Anisotropic diffusion (AD) proposed by Perona & Malik (1990) have contributed significantly to speckle-noise reduction. The most important thing is to differentiate the gradient between edges and noise. By doing so, the edges detail of the US image can be preserved but most of the AD methods cannot handle this problem efficiently and during the suppression of speckle they also lose the edges information.

The edges preservation during the speckle noise removal is still an open research area for researchers. It is highly beneficial to focus on further improving US knee joint cartilage images via the reduction of speckle noise. The main purpose of this research is to effectively preserve edges during diffusion for the speckle reduction of US images. Hence, a technique to apply to real US images is proposed and analysis of its performance over other existing methods is conducted.

1.2 Problem Statement

During the removal of speckle-noise using AD methods, the effectiveness of the method depends upon different factors like the strength to distinguish the gradient of edge from that of noise, the precision of the edge stopping function to stop the edge from over smoothing, and the ability to determine automatically the termination time of diffusion. It is noticed from the literature review that researchers have worked on AD methods to reduce the speckle noise, but these techniques mostly have limitations in edge preservation. The methods which perform better in edge preservation, but the diffusion functions still have limitation in terminating the diffusion process correctly.

Therefore, the proposed research aims to design a method which not only reduces the speckle noise but also preserves the edges effectively and automatically stops the diffusion when the desired results are obtained. To achieve the desired outcomes, the parameter settings of the AD filter is improved. Four gradient thresholds instead of one or two are included. It is also proposed that a conductance or diffusivity function which stops the diffusion near edges efficiently. Mean Absolute Error (MAE) is used as stopping criteria to control the number of iterations. The performance of the proposed approach is evaluated using four different evaluation metrics.

1.3 Objectives

1. To design and develop a technique for speckle noise removal from knee US images using anisotropic diffusion method.
2. To investigate the efficiency of the proposed method for the edge preservation of US images during speckle noise removal.
3. To compare and evaluate the performance of the proposed method with other methods for speckle noise removal.

1.4 Scopes of the Research

The scope of this study was to perform noise reduction and edge preservation from knee US images. The scope of this study includes but is not limited to:

- Collecting the knee images of thirty healthy volunteers with acceptable resolution.
- Simulating and testing the proposed algorithm using MATLAB software.
- Implementing the other well-known algorithms for the removal of speckle noise.
- Comparing other methods for benchmarking the proposed algorithm to ensure the better performance of the algorithm in terms of noise reduction and edge preservation.

1.5 Organization of the thesis

This thesis is organized into five main chapters. i) introduction; ii) literature review; iii) proposed methodology (iv) results and discussion and lastly v) conclusion and future recommendation. The contents of each section in the thesis are summarized as follows:

Chapter 1: This chapter explains the background of the topic and the importance of knee US. It also describes the problem statement which provides a base for the objectives of this study. According to the objectives of the study, the scopes of the current thesis are also explained.

Chapter 2: This chapter profoundly describes the literature review on speckle noise reduction. First, it gives an overview of different non-AD methods used for speckle noise removal. It also explains various AD methods and their performance in noise reduction and preserving the details of the edges.

Chapter 3: In this chapter, the methodology used to remove the speckle noise while preserving the details of the edge is discussed in detail. The scaling of diffusivity function and its comparisons with another diffusivity function is explained. The four gradient thresholds and MAE as stopping criteria to stop iterations are utilized in methodology.

Chapter 4: The comparison of the proposed model with other techniques is presented in this chapter. The performance of the proposed diffusivity function and the effect of four gradient thresholds are assessed. The overall performance of the proposed model is analyzed using subjective and four different objective evaluation metrics.

Chapter 5: This chapter summarizes the thesis work and recommends a few suggestions for future work improvements.

CHAPTER 2: LITERATURE REVIEW

2.1 Introduction

Ultrasound is the most widely used imaging technique for the analysis of knee cartilage. However, the diagnostic use of US images becomes difficult due to the low image quality of the US. One of the main reasons for this low image quality is speckle noise. This chapter reviews the work related to the removal of speckle-noise from US images to have a better and improved image for analysis.

2.2 Non-Anisotropic Diffusion Methods

To reduce the speckle noise early filters originated mainly to reduce the noise in Synthetic Aperture Radar (SAR). The most applicable filters for this purpose are Lee (Lee, Grunes, & Mango, 1991), Frost (Frost, Stiles, Shanmugan, & Holtzman, 1982) and Kuan (Kuan, Sawchuk, Strand, & Chavel, 1987). These filters have almost the same formation with a slight change in model assumption and the derivatives. The pixel values of the output image are calculated by applying a filter window on the pixel and calculating some linear combinations of pixel intensity in the window.

The balance in smoothing between homogenous regions and edges depends upon the coefficients of variation of the filter window. Frost (1982) attains a balance between homogenous and edges by forming an exponential shaped filter. This behaves as an identity filter and averaging filter on an adaptive basis. A few more filters also used the same approach of statistical filters (A. Lopes, Nezry, Touzi, & Laur, 1993; Armand Lopes, Touzi, & Nezry, 1990; Mandal, Satapathy, Sanyal, & Bhateja, 2017).

An unsharp masking filter proposed by Dutt & Greenleaf (1996) which smoothes the images based on statistics of log-compressed images. This filter was unable to remove the speckle around the edges of the image. Loupas, McDicken, & Allan (1989) proposed another filter named as an Adaptive Weighted Median Filter (AWMF) to replace the pixel value based on the traditional median filter. For replacement, the value of speckle must be smaller than half of the filter window size. Nevertheless, its ability to reduce the speckle is extremely sensitive to a few empirically determined parameters, particularly if a small window is used for the filter.

To overcome the shortcoming associated with statistical filters, the line segments technique is proposed in (Czerwinski, Jones, & O'Brien, 1999). They apply short line segments in different angular positions and choose the position and orientation of the line that is most probably characterizes the line in the ultrasound image. Still, this method suffers a compromise between speckle reduction and effective line improvement. However, this technique poses a trade-off between effective line enhancement and speckle reduction.

Several researchers (Chen, Yin, Flynn, & Broschat, 2003; Huang, Chen, Wang, & Chen, 2003; Karaman, Karaman, Kutay, & Bozdagi, 1995) proposed a filter which is based on region growing spatial filtering technique. The method is grounded on the assumption that pixels belong to the same region or object if these pixels have a similar grey level and contextually connected to each other. By using this theory pixels are divided into different groups and spatial filtering is performed in each group using local statistics. The core problem in applying these approaches is how to plan suitable similarity criteria for the region growing.

Although these non-AD based filters are referred to as edge-preserving, these filtering approaches have some major limitations. These filters do smooth in the homogenous region and stop smoothing near edges. Whenever there is an edge in the window of filter it will inhibit the smoothing. This process does not eliminate the speckle near edges. Secondly, the despeckle filters are not directional. Near an edge, all smoothing is disallowed while the correct method to remove speckle near edges that it must prevent smoothing in directions vertical to the edge and at the same time encouraging smoothing in directions parallel to the edge. Third, the thresholds used in the improved filters, even though driven statistically, are temporary enhancements that only validate the deficiency of the window-based methods. The hard thresholds that are calculated by measuring the average of the neighborhood and identity filtering cause the problem that in extreme cases averaging filter leaves the sharp features unfiltered at noisy boundaries. On the other hand, identity filtering in extreme cases leads to blotching artifacts from averaging filtering.

Different frequency-based methods are also used for despeckling US images. The most popular used procedure is wavelet-based methods. The multiplicative speckle noise is converted into additive noise when it is converted into a frequency domain. The wavelet coefficients are statistically modeled to remove the speckle noise (Amirmazlaghani & Amindavar, 2012). Penna & Mascarenhas (2019) used the Haar wavelet transform to remove the speckle noise from SAR images. As mostly the speckle follows gamma distribution, so they used stochastic distance for gamma distributions. An exponential polynomial is used to describe the Haar coefficients.

To remove the speckle noise using wavelet, the selection of threshold value is a very important step. Different Wavelet methods used various thresholding techniques. The thresholds coefficients are important as they not only play an important role in removing the noise coefficients but also used to recreate the image. By reviewing different thresholding methods, an adaptive thresholding technique is proposed to remove the noise efficiently from US images (Kulkarni & Madathil, 2019). The wavelet transform is faster and memory-efficient (Joel & Sivakumar, 2018). However, the performance of the wavelet becomes limited as speckle remains in low pass components and these never raise the signal to noise ratio as high compared to other methods (Joel & Sivakumar, 2018; Penna & Mascarenhas, 2019).

Recently, deep learning-based algorithms are also proposed by different researchers for the removal of speckle-noise from the medical images (Ker, Wang, Rao, & Lim, 2017;

K. Zhang, Zuo, Chen, Meng, & Zhang, 2017). A deep learning technique like a Convolutional Neural Network (CNN) is one of the most used architectures to remove speckles from SAR images. U-net is modified for the desired purpose (Lattari et al., 2019). The main obstacle in deep learning is that it requires a lot of labeled data for training which is not very much available in case of medical imaging. It also needs numerous tuning parameters for the training the model which makes it difficult to configure. Furthermore, most of the methods based on deep learning are considered for the removal of Gaussian noise and they cannot tackle speckle-noise very well (H. Yu, Ding, Zhang, & Wu, 2018).

2.3 Anisotropic Diffusion Based Methods

Nonlinear AD is a filtering technique based on Partial Differential Equations (PDE). It is used to remove the noise from the image by diffusion method and the smoothing of noise is characterized by linear and nonlinear diffusivity functions.

2.3.1 Perona-Malik (PM) Model

To remove the speckle noise from the images using AD, Perona & Malik (1990) introduce a new definition of scale-space called PM model. This modified definition of the previous linear scale-space model that was proposed by Hummel (1987). The method does not perform the uniform smoothing all over the image instead, it performs the smoothing within the region of preferences and stops diffusion process across the boundaries. The main problem is how to know the location of boundaries before applying the diffusion process. This task needs an estimator function $E(x, y, t)$ with the property that $E(x, y, t) = 0$ in the area of the image which is not boundary and $E(x, y, t)$ adopt some positive value at each edge point. So, the simplest estimation of edge position in any image is a gradient of the image. The gradient is a vector quantity, so it not only tells the largest possible change in intensity of image but also the direction of change. In the image, it is calculated by taking the derivatives in x and y-direction. Based on the above discussion, Perona and Malik suggested the following non-linear model for the reduction of speckle noise.

$$\begin{cases} \frac{\partial I}{\partial t} = div[c(|\nabla I|).\nabla I] \\ I(t=0) = I_0 \end{cases} \tag{2.1}$$

In Equation (2.1), I is the original image, div is the divergence operator. The estimator function is denoted by ∇ which is gradient operator. $c(\nabla I)$ is a function of the image gradient and it is known as diffusivity function/ stopping function/diffusion coefficient. The function c(.) is very important as the selection of this function will not only preserve but also sharpen the edges. Perona and Malik in their work proposed two types of diffusivity function.

$$c_1(|\nabla I|) = e^{-(|\nabla I|/k)^2} \tag{2.2}$$

and

$$c_2(|\nabla I|) = \frac{1}{1+\left(\frac{|\nabla I|}{k}\right)^2} \tag{2.3}$$

In the Equations (2.2) and (2.3), the contact "*k*" is a gradient threshold. The value of *k* has an important role in discriminating the gradients produced by noise and edges. Its value can be fixed either manually or using the "noise estimator". The value of *k* possesses the threshold role during diffusion. A large value of k values directs that the detected edges have large magnitude for the same soothing effect. But if the value of *k* is kept low, it will smoothen the weaker edges. Gradient magnitude $|\nabla I|$ is the key value for detecting the edges in an image. If the value of $|\nabla I|$ >> k, then diffusivity function $c(|\nabla I|) \to 0$ and out model turns into diffusion stopping and suppresses the diffusion. Conversely if $|\nabla I|$ >> k, then $c(|\nabla I|) \to 0$ then model encourages the diffusion as an isotropic diffusion and acts as a Gaussian filter. To select the gradient threshold automatically, PM used Canny's noise estimator. The discretized form of the PM model is given in Equation (2.4).

$$I_{t+1}(s) = I_t(s) + \frac{\lambda}{|\eta_s|} \sum_{p \epsilon \eta_s} c\left(\left|\nabla I_{s,p}\right|\right) \nabla I_{s,p} \tag{2.4}$$

In Equation (2.4) 'I_t *(s)*' is discretely sampled image and 's' symbolizes the pixel position in the discrete 2-D discrete grid. To get the optimum value the steps have to be repeated, so 't' is iteration steps, 'k' is the gradient threshold parameter and c is the conductance function. Here, $\lambda\epsilon(0,1)$ controls the diffusion rate, and η_s means the 4 neighborhoods spatial pixels of pixel s. Hence,$\eta_s = N, S, E, W$, where N, S, E, and W denotes the north, south, east, and west neighborhood of pixel s respectively and $|\eta_s|$ is equal to 4. Here the gradient operator ∇ indicates a scalar quantity which is the distance between the neighboring (p) and center pixel (s) in each direction. So, $\nabla \mathrm{I}_{s,p}$ can be represented as

$$\nabla I_{s,p} = I_t(p) - I_t(s), \qquad p\epsilon\eta_s = N, S, E, W \tag{2.5}$$

This technique is broadly used for image denoising, like in SAR images, Additive White Gaussian Noise contaminated images, and US images (L. Guo, Xu, Xu, & Jiang, 2015). An AD-based filter has been recently used for full polarimetric SAR image despeckling (Ma, Shen, Zhang, Yang, & Zhang, 2015).

The PM model overcomes the disadvantages of linear smoothing. The main problem in using the linear smoothing was that it does not only blur the edges but also removes the important details during the removal of speckle noise. PM model solves this problem but still compromises between noise reduction and edge preservation (Xu et al., 2019). This method mainly has two main drawbacks. First, if the signal is affected by white noise, a very large oscillation of gradient ∇I is introduced by the PM model. This effect fails the conditional smoothing of the model since the model looks at these noises as edges and hence does not apply smoothing (Nageswari, Rajan, & Manivel, 2017). Before applying the diffusion equation, the PM model also recommends the integration of low pass filters to smooth images. Still, a new parameter must be involved for adjustment and adoption again, which must be avoided by introducing an anisotropic filter. The second disadvantage is the type of diffusivity function used by the model. The diffusivity function $c(q) = e^{-q}$or $c(q) = (1 + q^2)^{-1}$ are based on no precise theory (Zhou, Guo, Zhang, & Wu, 2018). It should be examined to ensure that flow function *qc(q)* is incremental to ensure the existence and uniqueness of the diffusivity function (c), else the process becomes unstable.

2.3.2 Speckle Reducing Anisotropic Diffusion

Another method known as Speckle Reducing Anisotropic Diffusion (SRAD) was proposed by (Yongjian Yu & Acton, 2002). In this approach, they used statistical methods and used Lee and Frost filters (Frost et al., 1982) for removing the speckle in the homogenous region and preserving the edges. Lee filters based on the standard deviation of pixels values, designed for radar images to remove speckle noise and preserve the edges. Filter produced the enhanced data by using a linear speckle noise model and the Minimum Mean Square Error (MMSE). While Frost filter is a statistical filter that uses the local statistics of the sliding window to preserve the edges. The smoothness of the filter is controlled by the exponentially damped convolution filter. For removal of speckle noise, Yu and Acton used PDE of PM model and combine the PDE approach with the adaptive filters approach and proposed a new AD method for removal of speckle noise. Similarly, Choi & Jeong (2018) use the SRAD with a guided filter to remove the speckle noise. Even though these methods have a better ability to preserve edges compared with conventional AD methods, SRAD is often incompetent to yield a reasonable result in filtering US images (F. Guo et al., 2018).

2.3.3 Laplacian Pyramid Nonlinear Diffusion

The limitation of SARD overcomes by a method Laplacian Pyramid Nonlinear Diffusion (LPND) proposed by (F. Zhang, Yoo, Koh, & Kim, 2007). In this method, the laplacian pyramid is used. In the first step, image is transformed in the Laplacian pyramid domain and reducing the image by applying a low pass filter followed by a subsampling image by a factor of 2. Then up sample the image by zero-padding and multiply by a factor of 4. In this manner, different layers of the pyramid are generated. At the second step, the speckle noise at each layer of the Laplacian pyramid is suppressed by nonlinear diffusion filtering. This is a step where this method uses different denoising approach compare to other laplacian pyramid-based methods (Jain, Ray, & Bhavsar, 2019; Kunz, Eck, Fillbrandt, & Aach, 2003). The estimated gradient value is calculated using a gradient on a Gaussian lowpass-filtered and Equation (2.1) adopts the following shape.

$$\frac{\partial I}{\partial t} = div[c(|\nabla G(\sigma) * I|). \nabla I] \tag{2.6}$$

where σ is the standard deviation of a Gaussian filter. The author suggests slight change is the diffusivity function of Equation (2.3) and also used the following function

$$c_2(|\nabla I|) = e^{-(|\nabla I|^2/2k^2)} \tag{2.7}$$

But no significant improvement is achieved, and he finally confines to the diffusivity function of Equation (2.2) and (2.3). For estimating the threshold value k, the robust Median Absolute Deviation (MAD) estimator is used. However, if several key parameters are involved, this method suffers from high sensitivity and hence is not strong to reduce the speckle.

For removal of speckle-noise from molecular images, Ling & Bovikm(2002) proposed a median filter base approach with AD. They named it anisotropic median-diffusion filter as they used the median filter with the PM model. The equation represents this model.

$$I_{t+1}(s) = \ Median\ (\ I_{t+1}(s), W\ ) \tag{2.8}$$

where W is a window of a median filter. The areas in the image with a small gradient are smoothened while the areas with large gradient are left unchanged. The large gradient value indicates that either there is edge or noise in the image so if the gradient value is largely due to noise spikes, this noise is removed by the median filter. Conversely, the median filter will not affect the image if the gradient is generated by edges. In this way with every iteration step low noise is removed by diffusion and impulsive noise is smoothened by the median filter. These method works show very good results particularly for low-SNR molecular images and it does not consider the statistical characteristic of the speckle (Hou, Lv, & Chen, 2019). As a result, the robustness of the speckle reduction is degraded.

2.3.4 Nonlinear Complex Diffusion

Guy, Nir, & Yehoshua Y (2004) extend the nonlinear AD to a complex domain and introduce method Nonlinear Complex Diffusion (NCD). Optical coherence tomography images are used to analyze the method. The characteristics of forward and reverse diffusions are combined to overcome the drawbacks of the conventional PM model. In this model, a diffusion coefficient is a complex number and as the complex diffusion coefficient approaches to the real axis then the imaginary part of the equation serves as an edge detector.

2.3.5 Oriented Speckle Reducing Anisotropic Diffusion

Oriented Speckle Reducing Anisotropic Diffusion (OSRAD) was proposed by (Krissian, Westin, Kikinis, & Vosburgh (2007). In this technique, matrix anisotropic diffusion is added to standard scalar anisotropic diffusion. It uses the direction of the gradient and principal curvature direction for diffusion. This filter allows the strength of speckle adaptive diffusion to vary in the curvature and contour directions. The OSRAD filter performs almost like that of the SRAD filter.

2.3.6 Detail Preserving Anisotropic Diffusion

Aja-Fernandez & Alberola-Lopez (2006) proposed another filter Detail Preserving Anisotropic Diffusion (DPAD). This method based on the SRAD filter with a new diffusion function. The main focus was on statistics of signal and noise. In SRAD method diffusion and estimation of statistics are performed parallel while here these two processes are split to gain more stable estimation. First, it calculates the variation coefficients of noise and signal and then chooses the diffusion process to apply. The proposed filter and SRAD perform equally as long as statistics are estimated properly which highlights that proper determination of diffusion function depends upon the correct estimation of statistics. Nevertheless, DPAD continues the diffusion when the number of iterations is large, leading to over smoothed images.

Catté, Lions, Morel, & Coll (1992) demonstrated that the performance of the PM model is not efficient due to the proposed diffusivity functions of the model. The diffusivity function is inefficient in distinguishing the gradient generated by the noise and the image features in noisy images. This filter often blurs the images and amplifies the noise instead of preserving the edges and smoothing the noise.

2.3.7 Catte_PM Model

Diffusion Equation (2.9) was proposed by (Catté et al., 1992) to overcome the weaknesses of the PM model. The moderation of the PM model is named the Catte_*PM* diffusion model (Jinhua Yu, Tan, & Wang, 2010).

$$\begin{cases} \frac{\partial I}{\partial t} = div[c(|\nabla(G(\sigma) * I)|).\nabla I] \\ I(t=0) = I_0 \end{cases} \tag{2.9}$$

where ‘*G(.)*’ represents the Gaussian kernel function, and ‘*’ is a convolution operator. In Equation (2.9), before applying the diffusivity function, the first image is convolved with the Gaussian kernel. This model is unresponsive to a noise having the value smaller than $'\sigma$’ which improve the model performance as now the chance of noise to misinterpreted as the edge is reduced. The diffusivity function of the *Catte_PM* model is as follows.

$$c_1(|\nabla I|) = exp[-(|\nabla(G(\sigma) * I)|/k)^2] \tag{2.10}$$

$$c_2(|\nabla I|) = \frac{1}{1+(|\nabla(G(\sigma) * I)|/k)^2} \tag{2.11}$$

Numerous diffusivity functions can be applied in AD methods which benefit in differentiating the filtering results (Black, Sapiro, Marimont, & Heeger, 1998). Therefore, to improve the performance of these techniques it is very significant to select a suitable diffusivity function. Furthermore, the function should be scaled in a way that edges are preserved effectively. The diffusivity function proposed by the PM model in Equation (2.2) gives high priority to wide regions over small regions. However, the second diffusivity function in Equation (2.3) gives higher priority to high contrast edges than to the edges with low contrast.

Black et al (1998) proposed a diffusivity function that generates sharp edges with a short time of convergence. The diffusivity function is defined as follows:

$$c_3(\nabla I) = \begin{cases} \frac{1}{2}\left[1 - \left(\frac{\nabla(G(\sigma)*I)}{k\sqrt{2}}\right)^2\right]^2, & x \leq k\sqrt{2}, \\ 0 & otherwise \end{cases} \quad (2.12)$$

Two more diffusivity functions are proposed by (Kamalaveni, Rajalakshmi, & Narayanankutty, 2015; Jimin Yu, Zhai, & Yie, 2018) are represented in Equation (2.13) and (2.15).

$$c_4(\nabla I) = \frac{1}{1+\left(\frac{\nabla I}{k}\right)^{\alpha(\nabla I)}} \quad (2.13)$$

Where,

$$\alpha(\nabla I) = 2 - \frac{2}{1+\frac{\nabla I}{k}} \quad (2.14)$$

$$c_5(\nabla I) = \left\{1 - exp\left(\frac{-3.31488\, x\, k^8}{\nabla I^8}\right)\right\} \quad (2.15)$$

The c_4 and c_5 diffusivity functions are also based on diffusivity functions proposed by the PM model.

The flow function is used to characterize the total flow of generated brightness. It is defined in Equation (2.16).

$$\Psi(x) = c(x)x \quad (2.16)$$

where Ψ denotes the total generated brightness flow. The x=k is the location where maximum flow incurs. Black et al. compare the efficiency of the diffusivity functions by allowing the flow functions to three scaled c_1, c_2, and c_3 to reach at the same maximum value at the same point (for example, x=0.2, as shown in Figure 2.1), hence signaling the same amount of brightness. The three revised diffusivity functions (c_1, c_2, c_3) are as follows.

$$c_1(x) = exp\left[-\left(\frac{x}{k\sqrt{2}}\right)^2\right] \tag{2.17}$$

$$c_2(x) = \frac{1}{1+\left(\frac{x}{k}\right)^2} \tag{2.18}$$

$$c_3(x) = \begin{cases} 0.67\left[1-\left(\frac{x}{k\sqrt{5}}\right)^2\right]^2 & x \leq k\sqrt{5} \\ 0 & otherwise \end{cases} \tag{2.19}$$

In the Equations (2.17), (2.18) and (2.19) the notation '$x = \nabla I'$', and the gradient threshold is represented by 'k'.

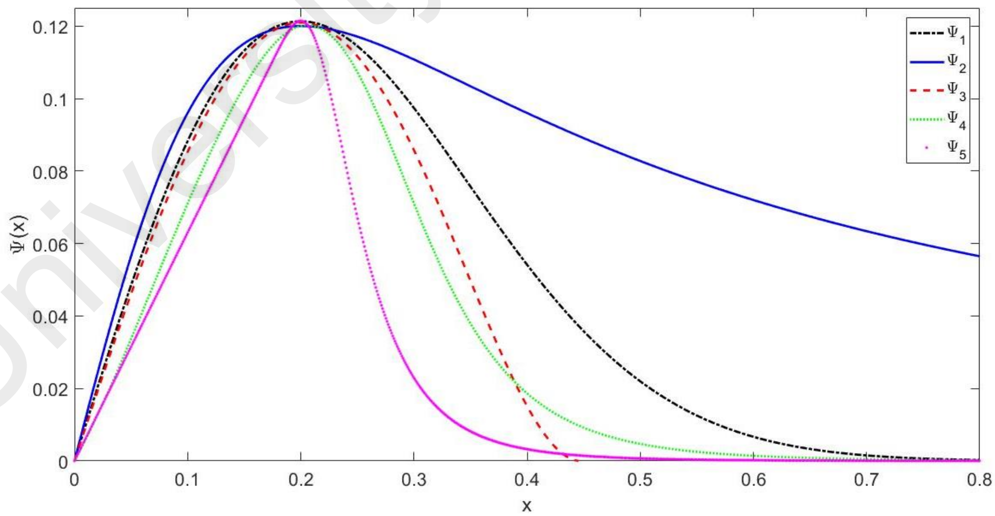

Figure 2.1: Flow functions of all five diffusivity functions

In Figure 2.1, the flow of the first two functions Ψ_1 and Ψ_2 is continuous and it smoothens the image. But if function Ψ_3 decreases after threshold to stop diffusion, which avoids the edges of the image from being over smoothed and becoming blurred. If an image having an edge threshold at $x = 0.4$ and analyze the behavior of all three diffusion functions, it can be seen from Figure 2.1 that the first two functions do not stop smoothing above $x=0.4$ yielding the image to be over smooth and blurred the edges. While the flow function Ψ_3 considers it an edge and stop diffusion. The behavior of Ψ_4 and Ψ_5 is also very similar to Ψ_3 and they do not also stop the diffusion exactly, but their values are very low near edges (e.g. x=0.4).

Given that c_3 prevents the edge from over smoothing by operating fast after a certain threshold, it is supported by scaling and comparison of function. Between the noise and edges, the point at x=0.4 is regarded as the threshold. Therefore, the gradient values higher or equal to x=0.4 are considered an outlier to stop diffusion, whereas those lower than x=0.4 smooth out the noise. In the comparison of the behavior of diffusivity functions, scaling of the flow function or diffusivity function is required to ensure that the values are zero at the exact point. For the flow function Ψ_2, a gradual decrease is observed; therefore, it is extremely effective for smoothing speckle noise but is inefficient in edge preservation.

The value of the gradient threshold also plays a vital role in effective edge detection. If the gradient threshold is overestimated, then the resultant image is over-smoothed. In addition, noise reduction ability is weakened due to the underestimation of the gradient threshold. Therefore, an optimum gradient threshold selection underpins the success in suppressing noise and preserving edges. As shown by Li & Chen (1994), the gradient threshold parameter must be a decreasing function of time to preserve edges beyond a predetermined threshold. In the PM model, only one gradient threshold is considered.
Different improvements in the AD models have been introduced by various researchers grounded on the earlier mentioned model (L. Guo et al., 2015; Jain et al., 2019; Terebes, Borda, Germain, Malutan, & Ilea, 2016). Mostly these models proposed some improvement in the basic method.

2.4 Summary

This chapter presents the methods and approaches used for reducing the speckle noise in images. The literature review has described previously used various non-isotropic diffusion techniques for speckle noise removal. The introduction of the AD method by Perona and Malik brings new research in this field. This chapter gave a review of different methods like SRAD, NCD, and DPAD, etc. which are based on the PM model. These methods used different diffusion functions and suggest different improvements in the PM model. The literature review has provided the background for the proposed methodology.

CHAPTER 3: METHODOLOGY

This chapter explains the proposed methodology to achieve the desired objectives. The diffusivity function, gradient thresholds and stopping criteria to stop the diffusion are discussed here. The evaluation matrices used for analyzing and comparing the performance of the proposed model with other models are also explained.

3.1 Dataset Description

The dataset of knee US images is obtained using an ultrasound machine ‘Aplio MX’, (manufacturer: Toshiba, State: Tochigi-Ken, Japan). Images of 30 different healthy volunteers were collected and professional sonographers performed the ultrasound scanning. The age group of twenty to thirty-five is focused on this study. The ratio of males and females 60% and 40%, respectively. The different sides like lateral and medial etc. of the knee joint were imaged to provide better observation of the cartilage of the knee joint. The 8MHz probe is used as the high-frequency probe can give better resolution of the image. The detection of smaller imaging particles is possible by using small wavelengths and hence high frequency.

MATLAB R2018b (MathWorks, 2018b) is used as a software for this project. The image processing toolbox has been installed and utilized. The computer that runs the MATLAB code is a personal HP laptop equipped with Intel(R) Core i5 2.3 GH CPU and 8 GB of memory.

3.2 Diffusion Model

The diffusion model used for the proposed method is

$$\begin{cases} \frac{\partial I}{\partial t} = div[c(|\nabla(G(\sigma) * I)|).\nabla I] \\ \quad I(t=0) = I_0 \end{cases} \tag{3.1}$$

Equation (3.1) was first presented by (Jinhua Yu et al., 2010). Before calculating the gradient and passing it to the diffusivity function, the first image is convolved with the

Gaussian filter. This is done to remove the additive noise so that additive noise is not misinterpreted with the edges. It requires the value of the standard deviation 'σ 'for the Gaussian filter. The window of different dimensions is used to find out the value of the standard deviation. The dimensions of 20×20 to 65×65 pixels are taken to automatically find out the standard deviation associated with the Gaussian noise present in the image. This window sizes are selected to have enough pixels to satisfy the statistical calculation. The standard deviation of the pixels of each block is calculated. From these calculated values, the block with most uniform pixels value is determined. The standard deviation of the most uniform block is taken as σ of the Gaussian filter. Determination of the size of the smoothing Gaussian filter by using σ is described in a study (Petrou & Petrou, 2010).

3.3 Diffusivity Function

As discussed earlier in Section 2.3.7, the smoothing ability of c_2 is very good but it lacks in terms of stopping the diffusion near edges. The diffusivity functions c_2 and c_3 are compared in this work. In the proposed model, the scaling of c_2 is performed. Scaling of the diffusivity function c_2 is accomplished in a way that Ψ_2 (flow function of c_2) tends to be zero or becomes very small after a predetermined threshold level e.g. at x=0.4. Therefore, it stops diffusion above x=0.4 and diagnoses it as an edge.

The basic concepts of digital image processing are utilized for choosing the scaling factor. When an image is represented digitally, usually 256 quantized levels are used to represents the image brightness. Therefore, for a digital image, digital 0 is equivalent to $\frac{0.5}{256} = \frac{1}{512}$. Generally, image enhancement is measured based on subjective evaluation. The subjective evaluation is measured by a human directly. Considering the subjective recovery of the image, the perceived change in greyscale by the human eye is considered. The human eye cannot differentiate less than 2 to 3 levels in 256 greyscale levels of the image. Based on this human eye capability of distinguishing between only a few levels, the numerical value of $\frac{1}{512} x 3 = \frac{3}{512}$ is adopted which is approximately equals to $1 + \frac{1}{(12.17)^2}$ at which $\Psi_2 = 0$. Giving the abovementioned statement, the conductance functions take the following shape.

$$c_2(x) = \frac{1}{1+\left(\frac{12.17x}{k}\right)^2} \tag{3.2}$$

In order to compare the two-diffusivity functions effectively, the c_3 is scaled so that both functions have the same maximum value. The c_3 diffusivity function is scaled and represented in Equation (3.3).

$$c_3(x) = \begin{cases} 0.13\left[1 - \left(\frac{x}{k\sqrt{5}}\right)^2\right]^2, x \leq k\sqrt{5}, \\ 0 \qquad\qquad\qquad\qquad otherwise \end{cases} \tag{3.3}$$

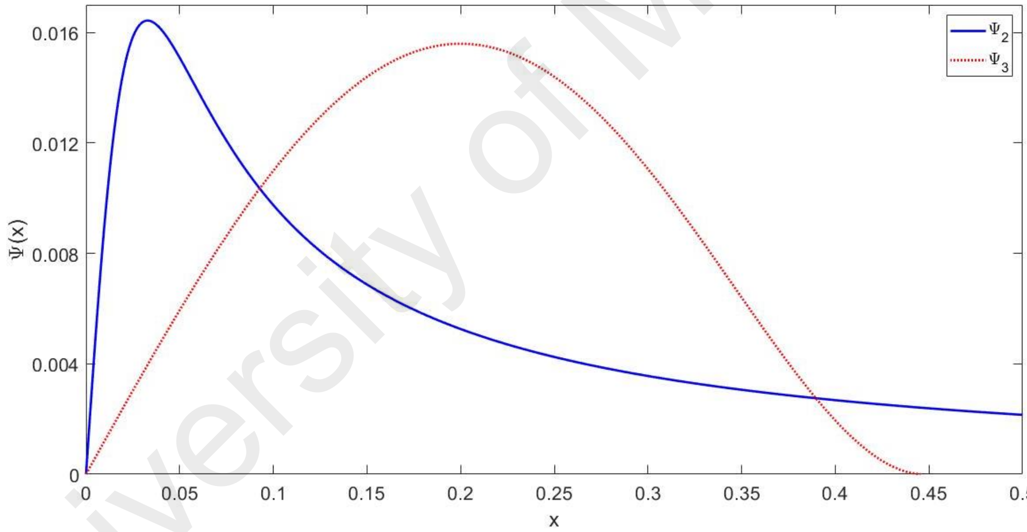

Figure 3.1: Comparison of flow functions of proposed diffusivity function with c_3 (Ψ_2 and Ψ_3)

In Equations (3.2) and (3.3) $x = \nabla I$ i.e. the gradient of image and k is the gradient threshold. When the value of flux goes to zero the part of the image is considered as edge and the diffusivity stops. This is demonstrated in Figure 3.1, when k =0.2 and x=k for the case of c_2 the value of flow function $c_2(x) = 0.006$ and $xc_2(x)$ is approximately zero. Therefore, the c_2 function detects it as edge and stops the diffusivity.

However, when $x<k$, the diffusion continues and smoothens the US image to reduce the speckle noise. In c_3, Ψ_3 is not zero, and the diffusion continues until $x \leq k\sqrt{5}$; when $x > \boldsymbol{k}\sqrt{\mathbf{5}}$, the diffusion stops, and it is considered as an edge or outlier. As shown in Figure 3.1, the flow Ψ_2 decreases more compared with Ψ_3, resulting in sharp discontinuities. Here, $\Psi_3=0$ when $x=0.4$. The value of Ψ_2 is less than 0.006 at $x=0.4$. As a result, the value of Ψ_2 can be assumed as zero at $x=0.4$ as observed in Figure 3.1. In fact, the value of Ψ_2 decreases rapidly and became zero before the value of x for which Ψ_3 is zero. In Figure 3.1, c_2 diffusivity function can perform better compared with c_3 (as c_2 descends faster and becomes zero before c_3 as shown in Figure 3.1). Therefore, diffusivity function c_2 is used for the reduction of speckle noise during the preservation of edges. The proposed diffusivity function c_2 is defined as

$$c_2(|\nabla I|) = \frac{1}{1+12.17*(|\nabla(G(\sigma)*I)|/k)^2} \tag{3.4}$$

3.4 Gradient Threshold

The PM model only utilizes four neighboring directions North, South, East and West of central pixel to compute the diffusivity function. This computation of the diffusivity function is not comprehensive enough as it does not consider other directions like NE, WN, WS, and SE. In order to solve this problem, the neighboring eight directions must be used to compute the diffusivity as shown in Figure 3.2 (b). So, the proposed method has $\eta_s = \{N, S, E, W, NE, WN, WS, SE\}$, where SE, WS, WN, and NE are south-east, west-south, west-north, and north-east neighborhood of the central pixel s, respectively.

$$\nabla I_{s,p} = I_t(p) - I_t(s), \text{ and } p \epsilon \eta_s = N, S, E, W, NE, WN, WS, SE \tag{3.5}$$

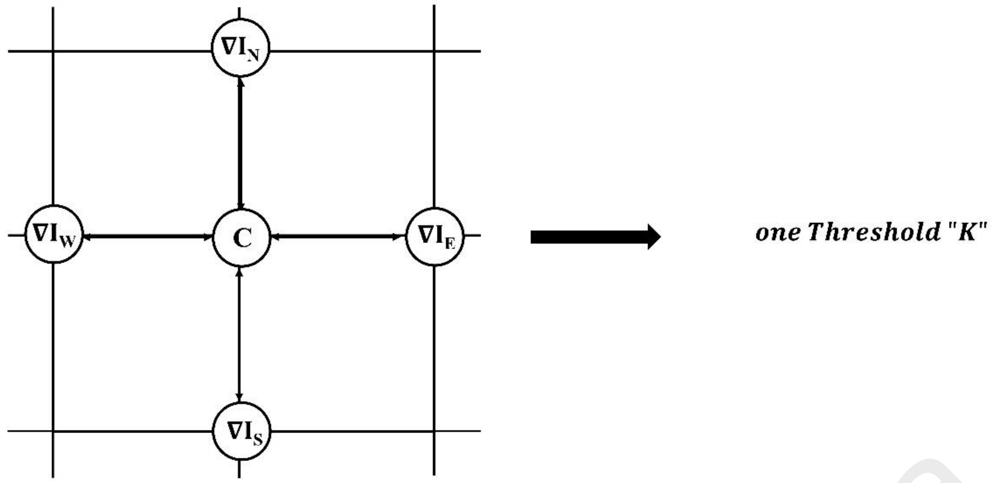

(a)

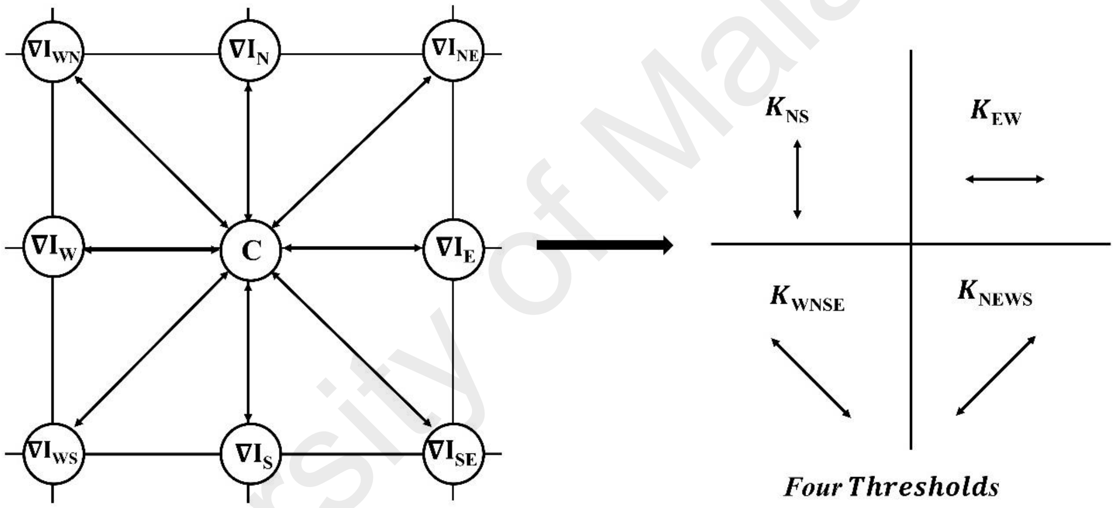

(b)

Figure 3.2: (a) One gradient threshold using four neighboring pixels (b) Four gradient thresholds using eight neighboring pixels

C is the central pixel (a) calculating one gradient threshold from four pixels in four directions (b) calculating four thresholds from eight pixels in eight directions. The difference between the brightness of central pixel s and every neighbor pixel in eight directions is computed using Equation (3.5). ∇ is defined as the scalar distance among the neighboring pixels based on this, the idea of eight different threshold parameters evolves, where the estimation of each threshold parameter accomplishes by using their differences in the eight directions. In a statistical sense, for the entire region of an image, it can be assumed that the absolute values of neighboring pixel differences of north and south direction are almost the same. Therefore, instead of considering two gradient thresholds for north and south, only one gradient threshold is considered. This regulation is also valid for west, east, west-south, north-east, south-east and west-north. Therefore, for the proposed method, the parameters of the four gradient thresholds are estimated. These are K_{NS}, K_{EW}, K_{WNSE} and K_{NEWS}. Here, K_{NS}, K_{EW}, K_{WNSE} and K_{NEWS} refers to the estimated gradient threshold in North-south direction, east-west direction, west-north and south-east direction, and north-east and west-south direction respectively.

3.4.1 Algorithm to Calculate Gradient Threshold

For the estimation of four gradient threshold parameters in each direction, the corresponding histogram of the absolute value of the gradient component is used. Knee algorithm is adopted to search the threshold between two populations. If the histogram has one peak and a long tail that fits with the straight lines, then the threshold can be estimated after the iterative process by observing the least square error. In this study, the gradients have long tail due to edges and steeper distributions due to noise. Hence the knee algorithm is an appropriate technique to calculate the thresholds. The details on the knee algorithm were described by (Petrou & Petrou, 2010). To calculate the threshold, a straight line is plotted by connecting the peak of the histogram to the point n bin on the right side of the peak towards the tail. Another straight line is plotted from the last bin of the histogram to the point n bins away on the left side of the last bin towards the peak. The intersection of two lines is the first estimated threshold value. The peak will be on the left of the threshold, so all points form threshold till peak is fitted using the least square error. The first line of the second iteration is plotted using inliers. Similarly, moving from threshold to the right-side same process is repeated and the second line of the second iteration is plotted. The intersection gives the second estimated threshold. This process is repeated for a few iterations and the final threshold is achieved.

3.5 Discretized Form of the Model

The discretized form using the eight gradient values is represented by Equation (3.6).

$$I_t = I_{t-1} + \frac{1}{\eta_s}[c(\nabla I_N, K_{NS})\nabla I_N + c(\nabla I_S, K_{NS})\nabla I_S + c(\nabla I_E, K_{EW})\nabla I_E + c(\nabla I_W, K_{EW})\nabla I_W + c(\nabla I_{WN}, K_{WNSE})\nabla I_{WN} + c(\nabla I_{SE}, K_{WNSE})\nabla I_{SE} + c(\nabla I_{WS}, K_{NEWS})\nabla I_{WS} + c(\nabla I_{NE}, K_{NEWS})\nabla I_{NE}] \quad (3.6)$$

where ∇I represents the gradient values and gradient threshold is represented by K. As mentioned in Section 3.4 that instead of calculating eight gradient thresholds in eight directions, only four gradient thresholds are considered in NS, EW, WNSE and NEWS directions. Thus, Equation (3.6) can be written as follow.

$$I_{T+1}(s) = I_t(s) + \frac{1}{|\eta_s|}\Big[\sum_{p\epsilon N,S} c(\nabla I_{S,P}, K_{s,p})\nabla I_{S,P} + \sum_{p\epsilon E,W} c\big(\nabla I_{s,p}, K_{s,p}\big)\nabla I_{s,p} + \sum_{P\epsilon NE,WS} c\big(\nabla I_{s,p}, K_{s,p}\big)\nabla I_{s,p} + \sum_{p\epsilon WN,SE} c\big(\nabla I_{s,p}, K_{s,p}\big)\nabla I_{s,p}\Big] \quad (3.7)$$

In Equation (3.7) for the first, second, third, and fourth $\boldsymbol{c(\nabla I_{S,P})}$, the estimated gradient thresholds are K_{NS}, K_{EW}, K_{NEWS}, and K_{WNSE}, respectively. Four gradient thresholds estimation provide more precise results in terms of edge preservation and noise reduction compared with one or two gradient threshold vectors in the continuous form. Given the variations in smoothing for each direction, results obtained from the experiment also exhibit good smoothing effects. In general, smoothing varies with different strengths in each direction. A high value of the K parameter is obtained in cases of a large difference in one direction compared with other directions. Hence, gradient threshold parameters also vary with the different strengths in each direction. In every iteration, the image quality and the values of the gradient threshold changes.

3.6 Stopping Criteria

The AD method is an iterative process and its performance also depends upon the number of iterations. It is very important to terminate the AD process after a certain number of iterations. The diffusion process can automatically be terminated by selecting a proper criterion to terminate the diffusion. Automatic stopping is crucial because the resultant image is blurred out in case the number of iterations is overestimated. On the other side underestimation of the iteration number causes unsatisfactory noise suppression. Mean Absolute Error (MAE) is an efficient stopping condition, used in AD to automatically stop the diffusion between two successive diffusion iterations (F. Zhang et al., 2007). To follow this method, the exponential drop in the MAE value is checked constantly with the increment of the iteration numbers. The diffusion process is stopped when the MAE value is less than a specific threshold to signal between the two iterations. In the proposed method the MAE stopping criteria are used due to its effectiveness in US images. Equation (3.8) is used to compute the MAE value in each iteration. Diffusion is stopped when the value is small enough.

$$MAE(I_t) = \frac{1}{m \times n} \times \sum_{(i,j)=1}^{m,n} \left| I_t^{i,j} - I_{t-1}^{i,j} \right|, \tag{3.8}$$

where $I_t^{i,j}$ and $I_{t-1}^{i,j}$ denote the filtered values of the pixel (i ,j) for time t and t-1, respectively. Here, n and m are the columns and rows of the diffused images, respectively. The edge information and tissue structure are characterized by the region of the diffused images. In cases of low and stable MAE values, the diffusion terminates to protect the diffused images from over smoothing.

Table 3.1 represents all the parameters with their specified functions and algorithm name, used for the proposed model.

Table 3.1: Parameters and specifications of the proposed model

Parameters	**Specifications**
Additive noise removal	Gaussian Filter
Diffusivity function	$\frac{1}{1+\left(\frac{12.17x}{k}\right)^2}$
Number of gradients	Eight gradients from all neighbor pixels of the center pixel
Gradient Threshold Algorithm	Knee algorithm
Number of gradient thresholds	Four (NS, EW, NEWS, WNSE)
Stopping criteria	Mean Absolute Error

The flow of the proposed model is shown in Figure 3.3. It completely explains the whole methodology steps in sequence.

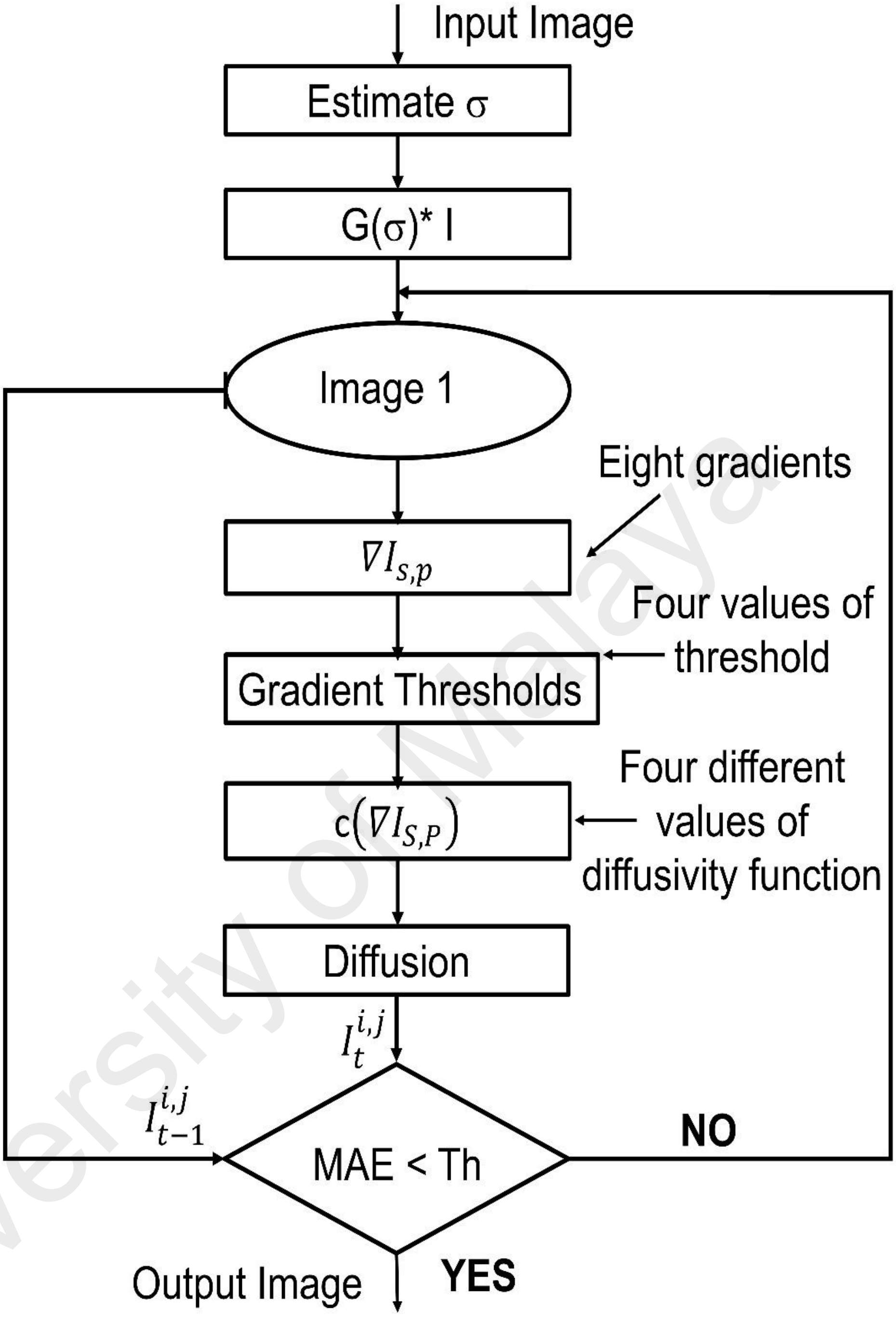

Figure 3.3: Flow chart of the proposed methodology

3.7 Evaluation Metrics

For evaluating the performance of the proposed method, four different evolution matrices i.e. Peak Signal-to-noise Ratio (PSNR), Structure Similarity Index Measurement (SSIM), Figure of Merit (FOM), and Equivalent Number of Looks (ENL) are used.

3.7.1 Peak Signal to Noise Ratio

PSNR is the measure of the reduction of speckle-noise from noisy images (Tsiotsios & Petrou, 2013). The commonly used unit for PSNR is the decibel (dB). A high PSNR value indicates a larger amount of speckle noise reduction. For calculating the PSNR, another important parameter Mean Square Error (MSE) is to be measured first. This parameter calculates the square of the difference of pixels between two images and then takes the average of all differences. The MSE is calculated using the Equation (3.9).

$$MSE = \frac{1}{M \times N} \sum_{(i,j)=1}^{M,N} \left(I_t(i,j) - I_0(i,j) \right)^2 \tag{3.9}$$

In Equation (3.9), I_0 denotes the original image, It represents the filtered image, M and N are the numbers of rows and columns in the image and (i,j) is the spatial location of the pixels. The MSE and PSNR have an inverse relation. If the value of MSE is high PSNR will be low and vice versa. After calculating the MSE numerical value, PSNR can be calculated using the following equation.

$$PSNR = 10 \, log_{10} \frac{max(I_0)^2}{MSE} \tag{3.10}$$

3.7.2 Structural Similarity Index Measure

SSIM is a perceptual evaluation metric that computes the image quality of the image after applying any processing on the image. It measures that how much information a human visual system has adopted from a scene in an image. Here, structure, luminance, and contrast are considered for the measuring criteria. The metric is used for the measurement of the preservation ability of important details in US images. The equation of SSIM is

$$SSIM = [c(I_t I_0)]^{\alpha} \times [l(I_t I_0)]^{\beta} \times [s(I_t I_0)]^{\gamma} \tag{3.11}$$

where *l*(.) denotes the luminance comparison function, *c*(.) is the contrast comparison function, and *s*(.) is the structure comparison function. Here, α, β, and γ is used to indicate the relative importance of these three components. Generally, $\alpha=\beta=\gamma=1$. The individual comparison of each measuring criteria is calculated using Equation (3.12).

$$SSIM(x, y) = \frac{(2\mu_x\mu_y + q_1)(2\sigma_{XY} + q_2)}{(\mu_x^2 + \mu_y^2 + q_1)(\sigma_x^2 + \sigma_y^2 + q_2)} \tag{3.12}$$

where μ_x and μ_y represents the average value of pixel *x* and *y*, respectively. The variances of *x* and y are denoted by σ_x^2 and σ_y^2, respectively and σ_{XY} represents the covariance of *x* and *y*. q_1 and q_2 are the constants used to stabilize the division with weak denominator. The range of SSIM value is 0 to 1, where 1 shows exactly similarity between images. So higher value represents that image details are preserved efficiently. The comprehensive discussion about the parameters setting is explained in (Z. Wang, Bovik, Sheikh, & Simoncelli, 2004; Zhou Wang, Simoncelli, & Bovik, 2000; F. Zhang et al., 2007).

3.7.3 Figure of Merit

FOM is a performance measure for comparing the images in terms of edge preservation. Equation (3.13) is used to calculate the FOM.

$$FOM = \frac{1}{ma\,x\,N_{real}, N_{ideal}} \sum_{i=1}^{N_{real}} \frac{1}{1 + d_i^2 e} \tag{3.13}$$

N_{ideal} is the total number of actual edge pixels i.e. those edge pixels found in the original image, and the number of detected edge pixels is N_{real}. The d_i symbolizes the Euclidean distance between *i*th nearest ideal edge pixel and detected edge pixel. The constant *e* is scaling constant or scaling factor. The numerical value of the constant *e* is 1/9 in literature. If the edge is localized but offset from the actual position, then the value of e can be adjusted for penalizing edge. The value of *e* used in the experiment is 1/9 (University of tartu, 2014). FOM is described by (Yongjian Yu & Acton, 2002). FOM varies from 0 to 1 and edge detection capability increases with the increase in the value of FOM.

3.7.4 Equivalent Number of Look

ENL is another significant metric for computing the ability of speckle-noise reduction (B. Wang, Chapron, Mercier, Garello, & He, 2011). A large value of ENL shows that the method has reduced the speckle noise efficiently from the US image. The size of the region of the image affects the value of ENL. Theoretically, a large area gives higher ENL value as compared to a small area by trading off the accuracy of readings. On approach to solving this is to divide the image into the 25×25-pixel region and calculate the ENL value of each region. The final value of ENL is determined by taking the average of ENL for all the small regions. In this experiment, The ENL of every image is calculated by dividing them into the 25×25-pixel region. The final value can be calculated by using the following Equation (Gagnon & Jouan, 2004).

$$ENL = \left(\frac{Mean}{Standard\ Deviation}\right)^2 \tag{3.14}$$

3.8 Summary

In this chapter, details of the proposed methodology to reduce the speckle noise and preserve edges are explained. Scaling of diffusivity function c_2 is performed so that it can stop the diffusion efficiently near edges. In addition, the four gradient thresholds are proposed to preserve the edges from all directions. The process will stop based on the MAE value. The metrics used to evaluate the performance of the method are also discussed.

CHAPTER 4: RESULTS

4.1 Introduction

This chapter presents the results of the proposed anisotropic diffusion method for speckle noise removal. First, the effect of introducing four gradient thresholds in the model and its simulated results are presented. Then, the performance of the proposed model and gives numerical results of evaluation matrices are stated. Four different evaluation matrices PSNR, SSIM, FOM, and ENL are used to analyze the proposed method.

4.2 Diffusivity Function

First, the results of the proposed diffusivity function are analyzed. For this purpose, a simulated image is utilized to assess the ability of noise removal of the proposed c_2 diffusivity function. Both c_2 and c_3 diffusivity functions are used to remove noise from the simulated image and results are shown in Figure 4.1. The original image is shown in Figure 4.1 (a). Different level of speckle-noise is added in images to observe the performance of c_2 over c_3 at multiple noise levels. Figure 4.1(b) from top to bottom represents the simulated noisy images having different levels of speckle noise. The top figure contains a very large amount of noise (σ= 0.1), the middle part has a variance of 0.05 while the bottom has the least noise level (σ= 0.02). The proposed model is applied to all simulated noisy images. Figure 4.1(c) and (d) show the output image using c_3 and c_2 diffusivity functions respectively. It is clear from the figures that c_2 reduce the speckle noise much better than c_3 function at different noise levels.

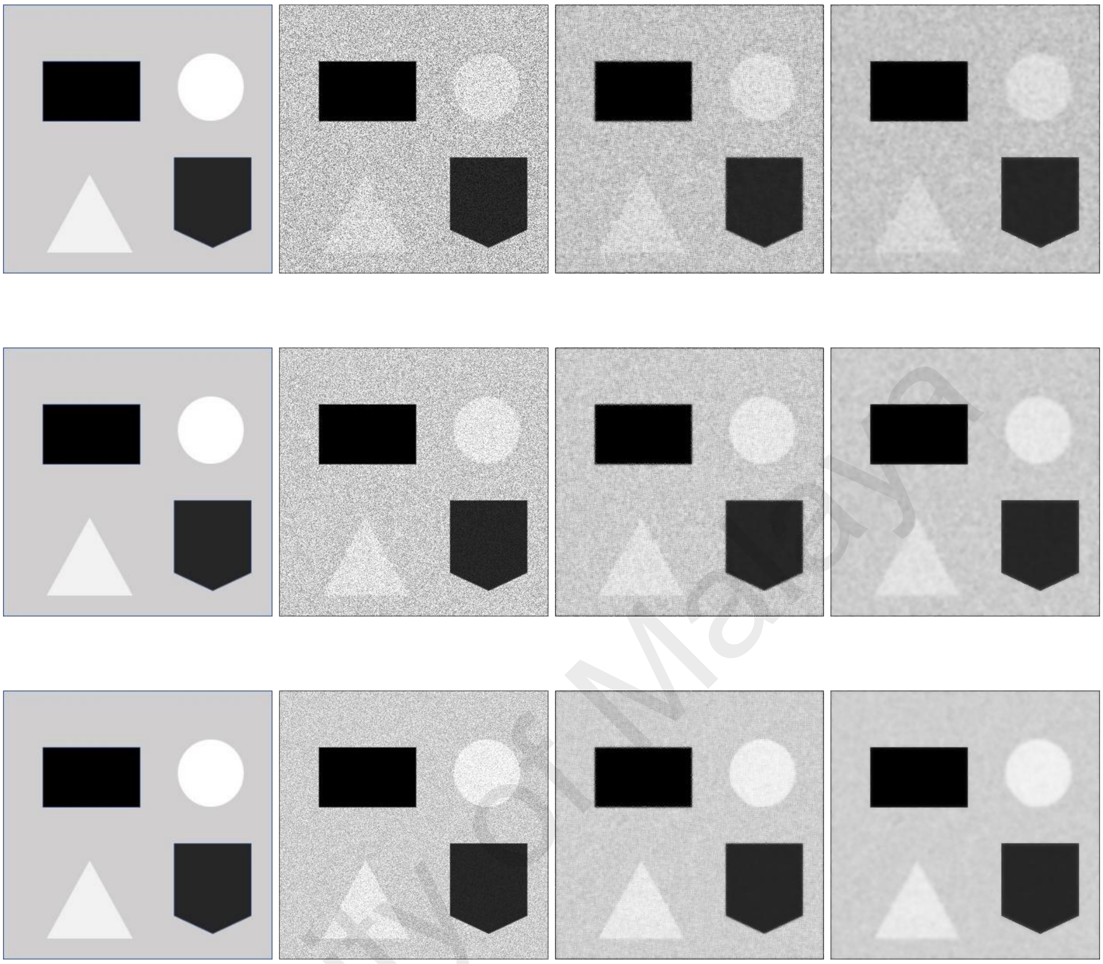

(a) (b) (c) (d)

Figure 4.1: (a) Original image (b) Simulated images with a high, medium and low variance of noise (c) Performance of proposed method using c_3 (d) Performance of proposed method using c_2

4.3 Gradient Threshold

As mentioned in Section 3.4 that four gradient thresholds are proposed for the reduction of speckle noise and preservation of edges. Seismic images are used for AD filtering with one, two, and four gradient thresholds to show the advantages of using four gradient thresholds over one or two. The reason for using the seismic image is that the visual perception for edge preservation of these images is better than US images. Hence, for analyzing the edge preservation capability of four gradient thresholds, seismic image is used. Figure 4.2 (a) represents the noisy seismic image, and Figure 4.2 (b), (c) and (d) represent the output images of AD filtering by using one, two and four gradient thresholds, respectively. If the lines in Figure 4.2 (a) and (b) are compared, the middle lines which are very week edges are considerably blurred. While these lines are prominent in Figure 4.2 (d). This phenomenon can also observe in other places in the images. It is clear from Figure 4.2 that the edge preservation in using four gradient thresholds is better than using one or two gradient thresholds. The threshold value between true edge and noise is overestimated by selecting one or two gradient threshold which leads to degradation of the image edge. From these observations, it is inferred that the proposed technique is better than other techniques in preserving edge while reducing the speckle noise of the US image because it uses four gradient thresholds instead of one.

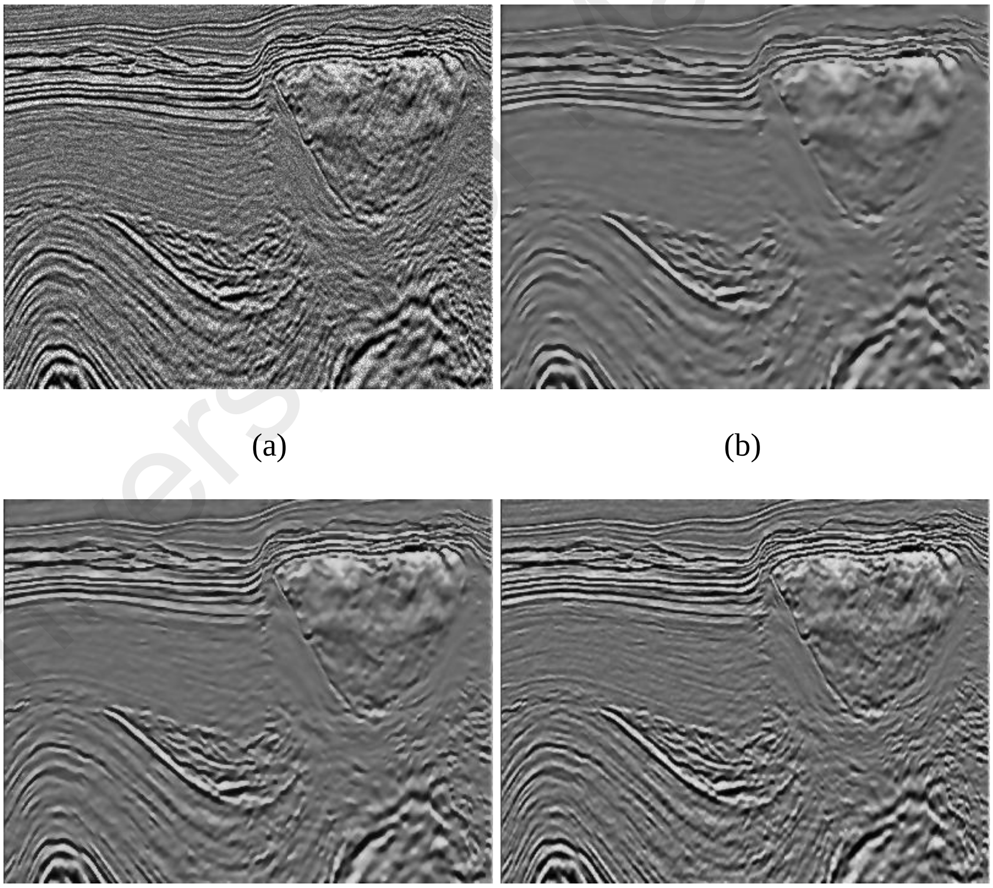

(a) (b)

(c) (d)

Figure 4.2: (a) Noisy seismic image. Output image of the filter using (b) one, (c) two, and (d) four gradient thresholds

The number of iterations plays an important role in determining the gradient threshold values. As the performance of the method is good if the gradient threshold value is decreasing the function of a number of iterations. The drop in gradient threshold values using one, two and four gradient thresholds are represented in Figure 4.3. In the case of only one gradient threshold is calculated for the entire process, the value of the threshold is very high. Thus, it performs high smoothing in homogenous regions and did not consider diagonal edges very much. The value of two gradient thresholds is lower compared to one as the value of K_{NS} and K_{EW} is less than K. Four gradient thresholds are calculated and only one among the four is shown in Figure 4.3. The gradient threshold estimated for K_{WNSE} in every iteration is observed and it has very low values compared to K_{NS}, K_{WE}, and K. This is because most edges of the image shown in Figure 4.2 are oriented in the direction from WS to NE. A large distance in that direction would result in high *K* values.

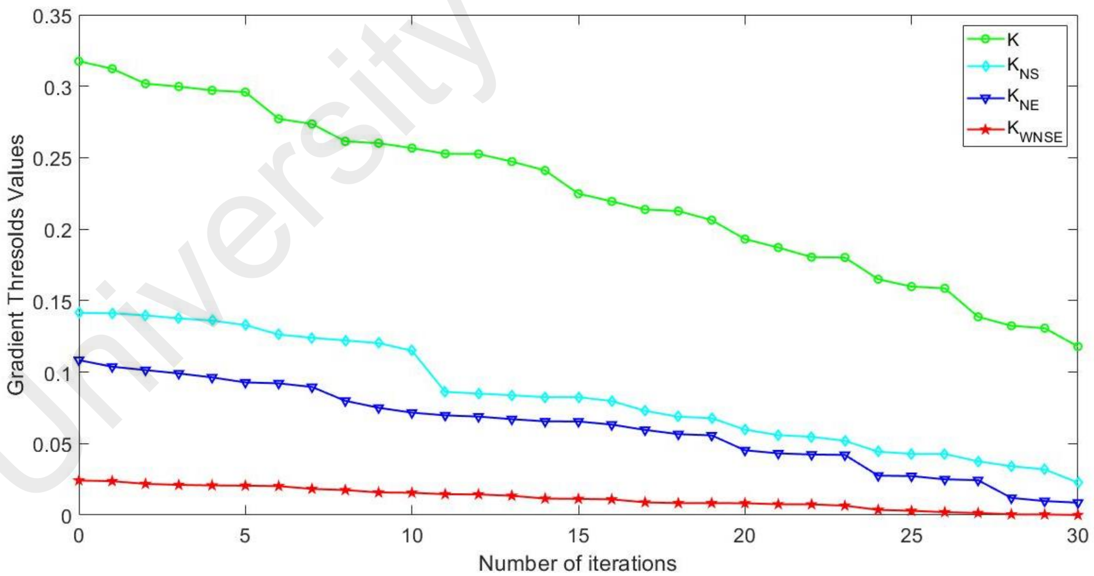

Figure 4.3: one (K), two (K_{NS}, K_{EW}), and one example from four (K_{WNSE}) gradient threshold.

4.4 Qualitative Analysis

Figure 4.4 (a) shows the medial side of the knee joint cartilage of the original US image. The images after filtering through different methods are shown in Figure 4.4 (b) to (h).

Figure 4.4 (b) is the outcome after filtering the image through the PM model. The noise removal is not very significant and also the edges become a blur. The output of the LPND filter is shown in Figure 4.4 (c). This output has better noise removal ability compare to PM model but still, edges are not well preserved. The NCD method has almost the same noise removal ability as LPND but this method preserves the edges better compare to LPND and PM model as shown in Figure 4.4 (d). The performance of SRAD and OSRAD are equally in terms of noise removal but OSRAD improved the SRAD in terms of edge preservation as depicted in Figure 4.4 (e) and Figure 4.4 (f). The DPAD method has an edge in noise removal over all previously mentioned techniques but edge preservation ability is almost the same as OSRAD. The output result of DPAD is represented in Figure 4.4 (f). The wavelet method has a deficiency in removing the noise components at the low level that is why is SNR never raises too much as shown in Figure 4.4 (h). In all the above methods either the edge, preservation ability is degraded due to over-smoothening which indicates that the gradient threshold is overestimated or the right side of ‘V’ shape cartilage is blurry and unclear. The resultant image after applying the proposed AD method is represented in Figure 4.4 (i). It can be noticed that in the output image of the proposed method “V” shape cartilage layer is significantly clear. Therefore, with the help of four gradient thresholds and diffusivity function, speckle noise is reduced during the edge preservation of US images.

Similarly, Figure 4.5 (a) represents the original US image of the knee joint of the lateral side. Figure 4.5 (b) to (h) are the output of the PM model, LPND, NCD, SRAD, OSRAD, DPAD and wavelet methods respectively. The image in Figure 4.5 (i) is the output of the proposed method g four gradient thresholds. The layer of reversed “U” shape cartilage is clear. From the resultant image in Figure 4.5 (i), the preservation of edge and reduction of the speckle-noise ability of the proposed method is clear.

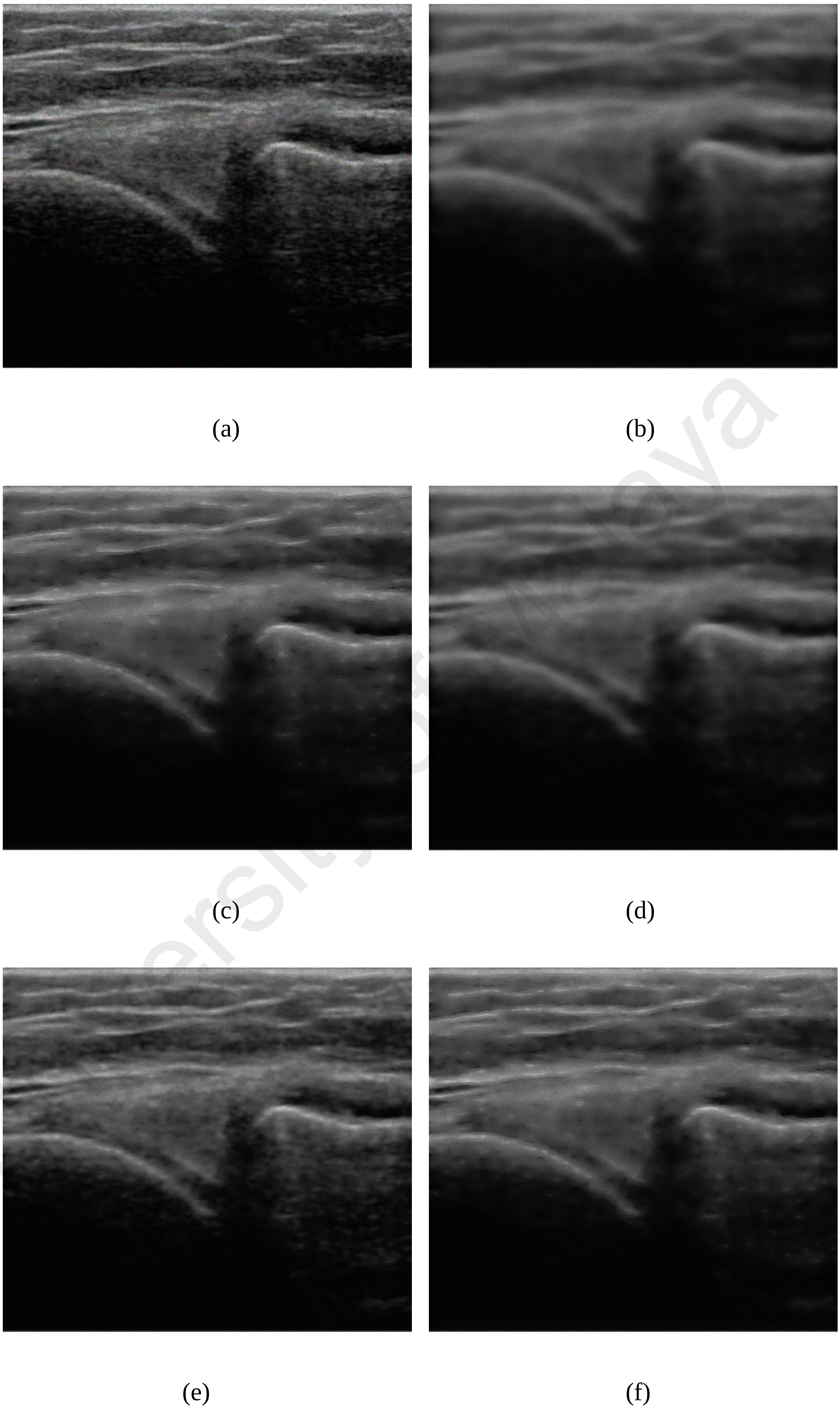

Figure 4.4: Medial Side of US image of knee joint cartilage (a) Original Image. AD filtered images by using (b) PM model (c) LPND (d) NCD (e) SRAD (f) OSRAD

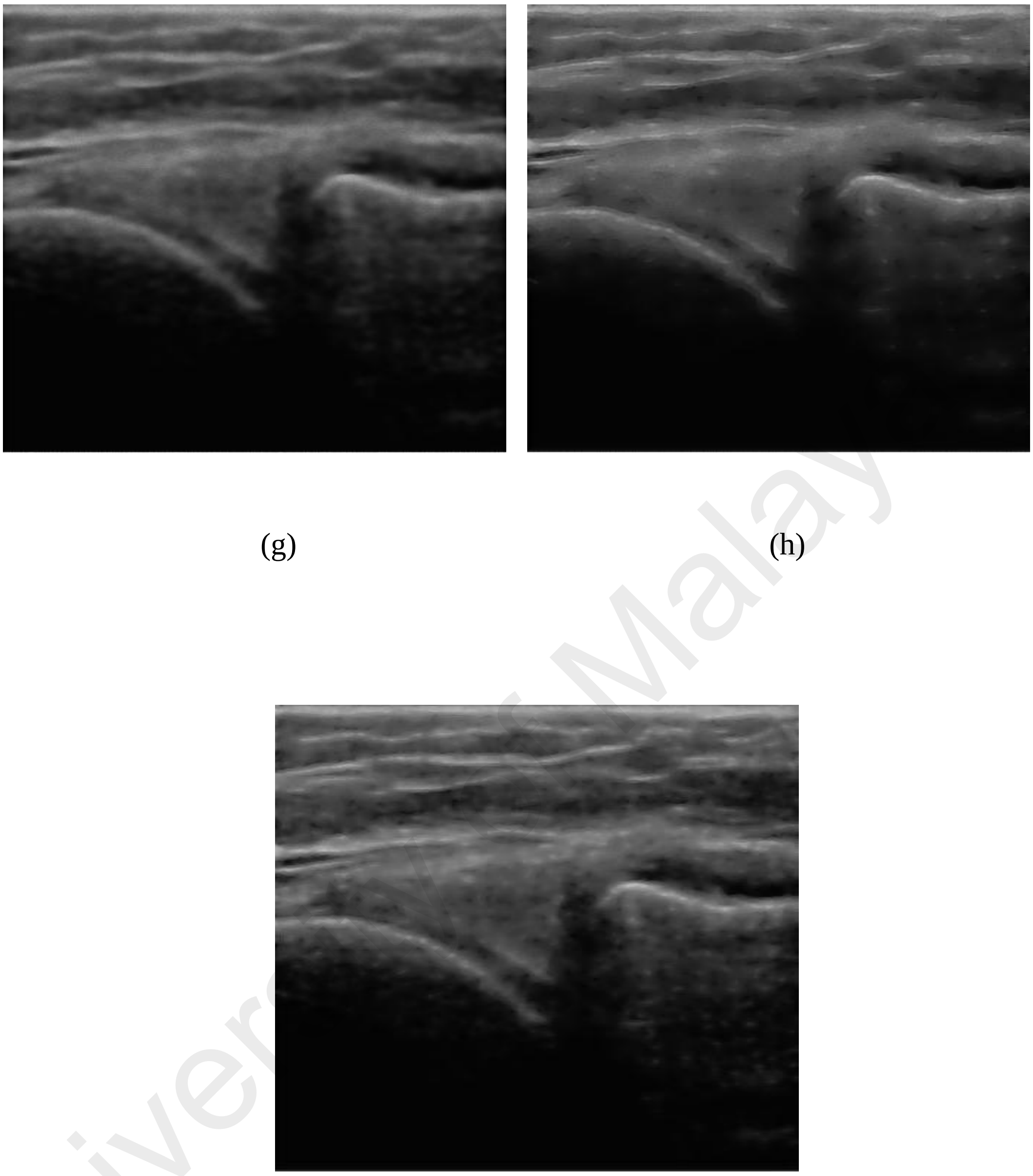

(g) (h)

(i)

Figure 4.4, continued: AD filtered images by using (g) DPAD (h) Wavelet (i) proposed Model

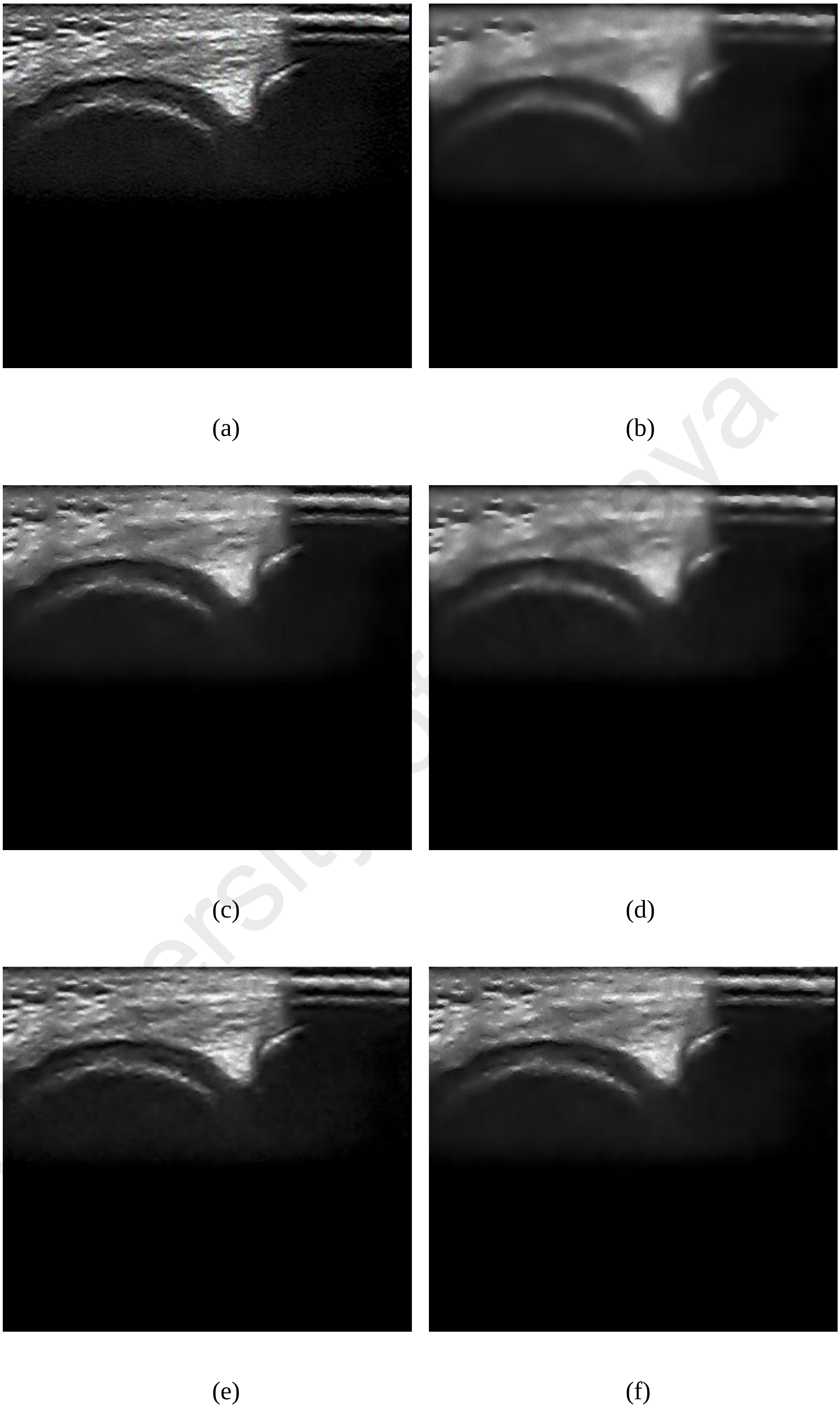

Figure 4.5: Lateral Side of US image of knee joint cartilage (a) Original Image. AD filtered images by using (b) PM model (c) LPND (d) NCD (e) SRAD (f) OSRAD

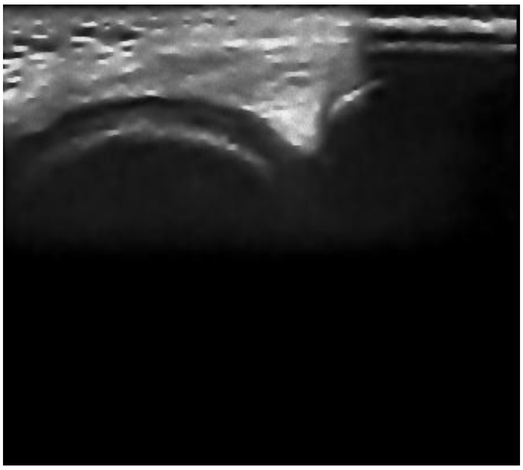

(g)

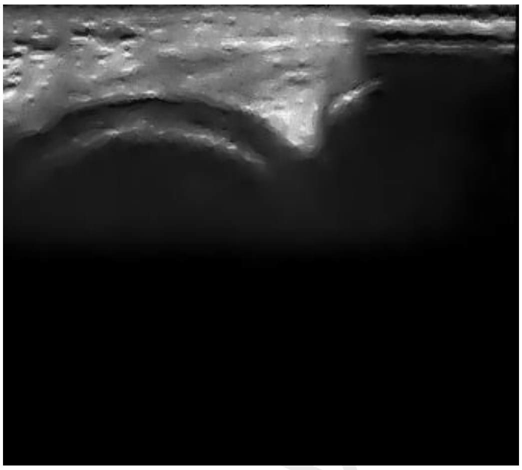

(h)

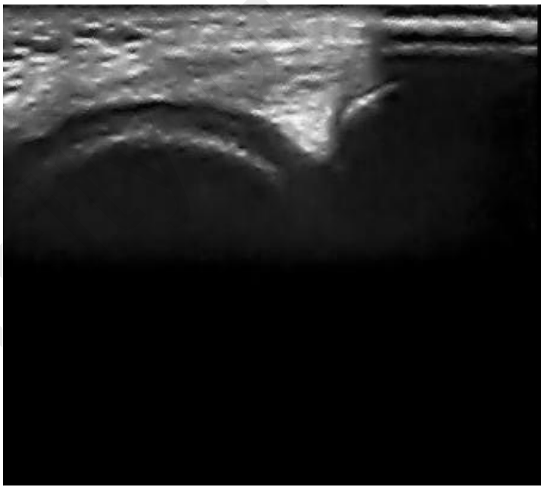

(i)

Figure 4.5, continued: AD filtered images by using (g) DPAD (h) Wavelet (i) proposed Model

Among the thirty images, Figure 4.6 to Figure 4.11 shows the few samples of different views of the knee US. This is clear from all images that the proposed model not only removes the speckle-noise but also preserves the edges.

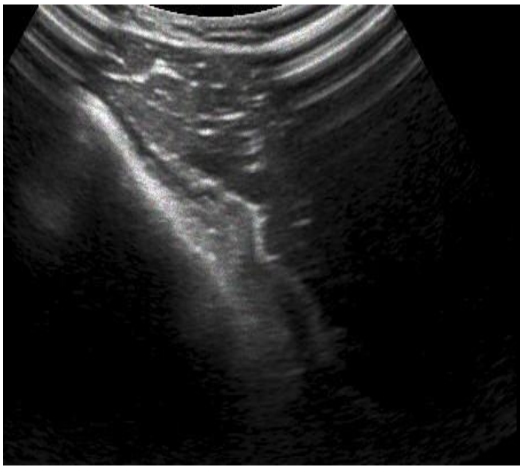

(a)

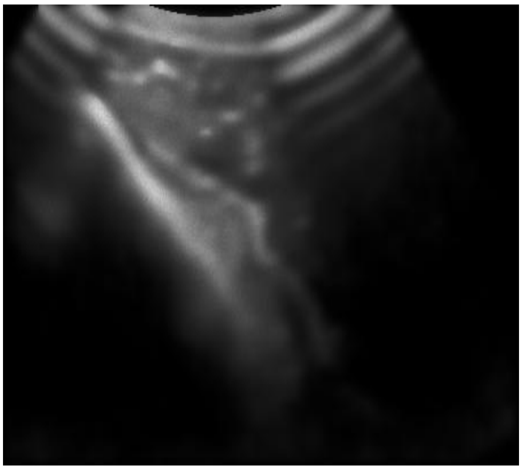

(b)

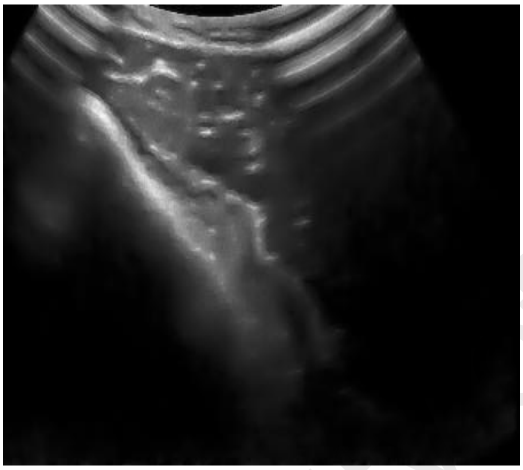

(c)

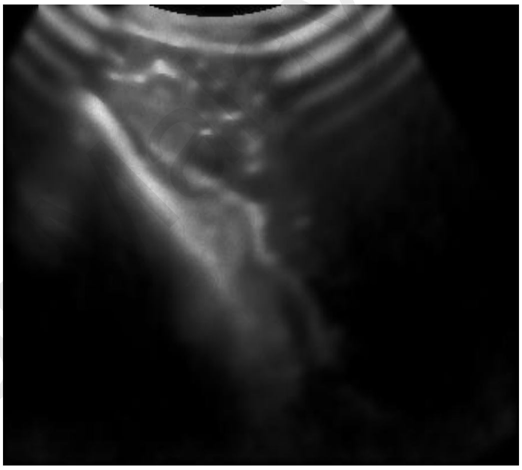

(d)

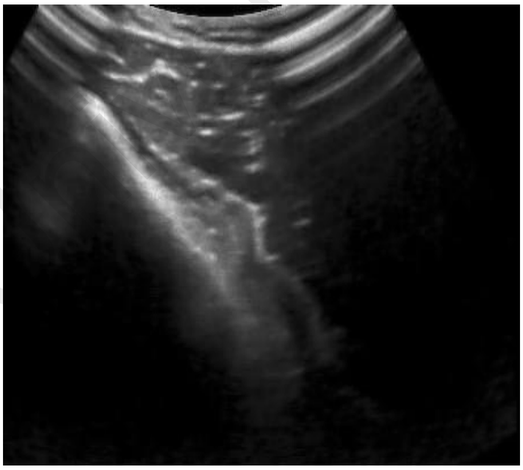

(e)

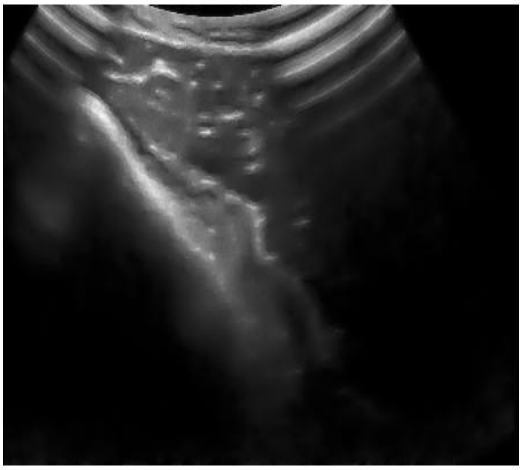

(f)

Figure 4.6: Third example of US image of knee joint cartilage (a) Original Image. AD filtered images by using (b) PM model (c) LPND (d) NCD (e) SRAD (f) OSRAD

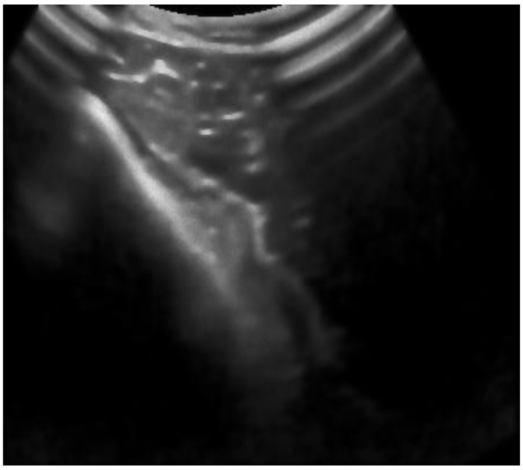 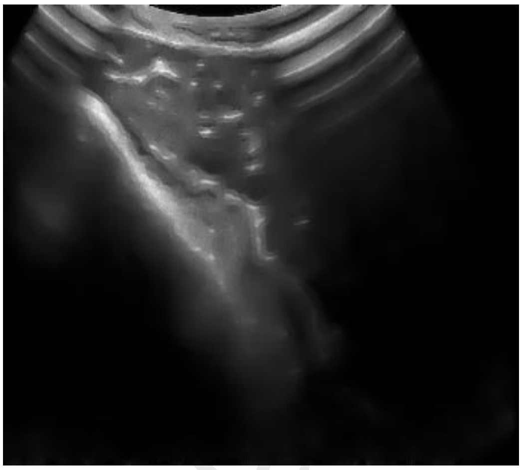

(g) (h)

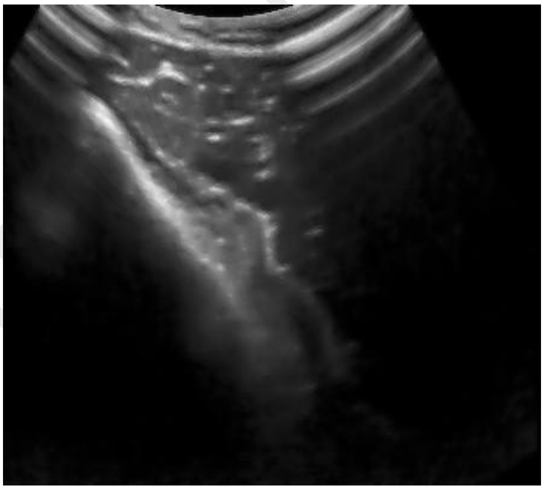

(i)

Figure 4.6, continued: AD filtered images by using (g) DPAD (h) Wavelet (i) proposed Model

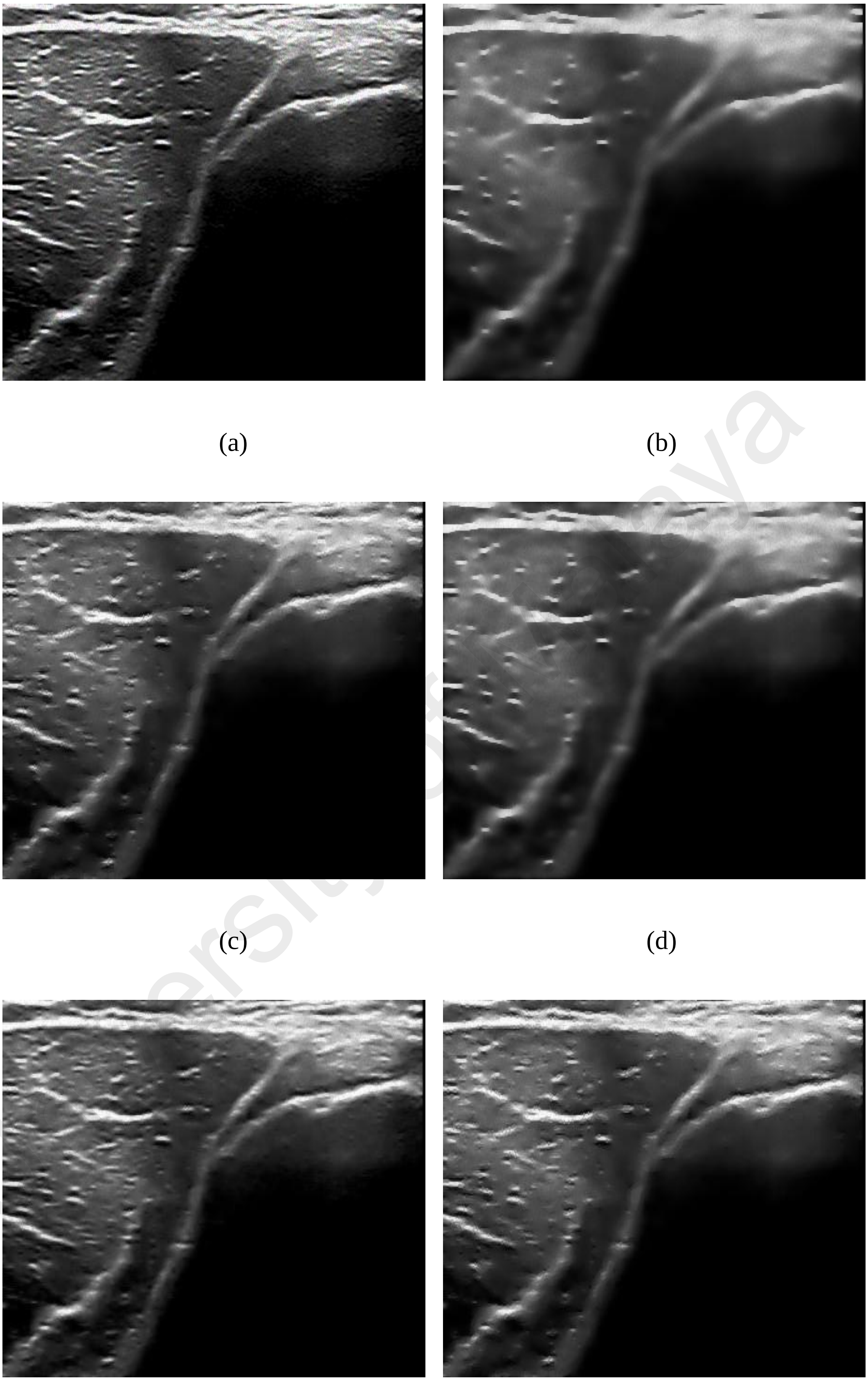

Figure 4.7: Fourth example of US image of knee joint cartilage (a) Original Image. AD filtered images by using (b) PM model (c) LPND (d) NCD (e) SRAD (f) OSRAD

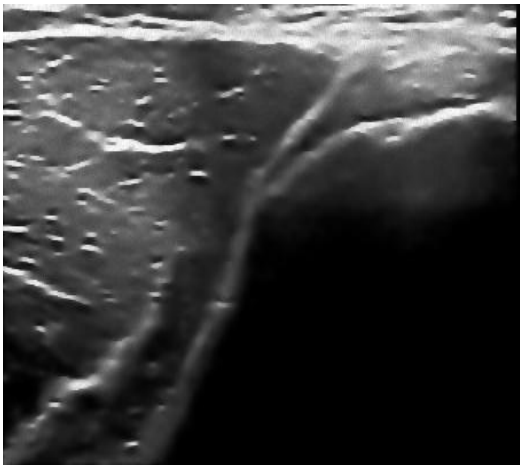

(g)

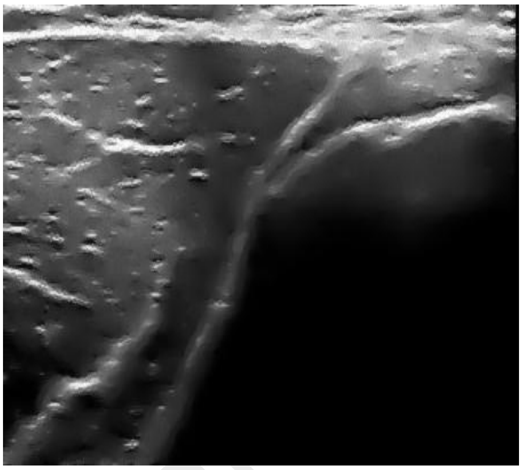

(h)

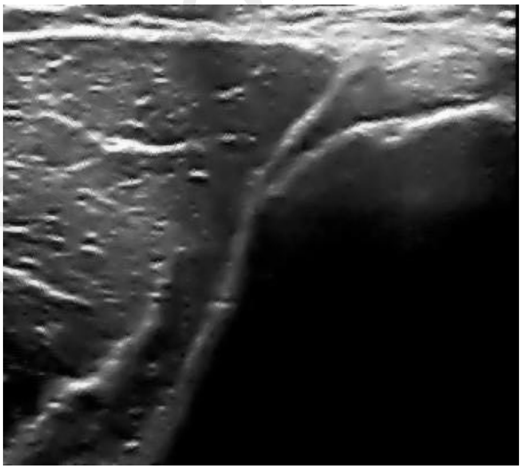

(i)

Figure 4.7, continued: AD filtered images by using (g) DPAD (h) Wavelet (i) proposed Model

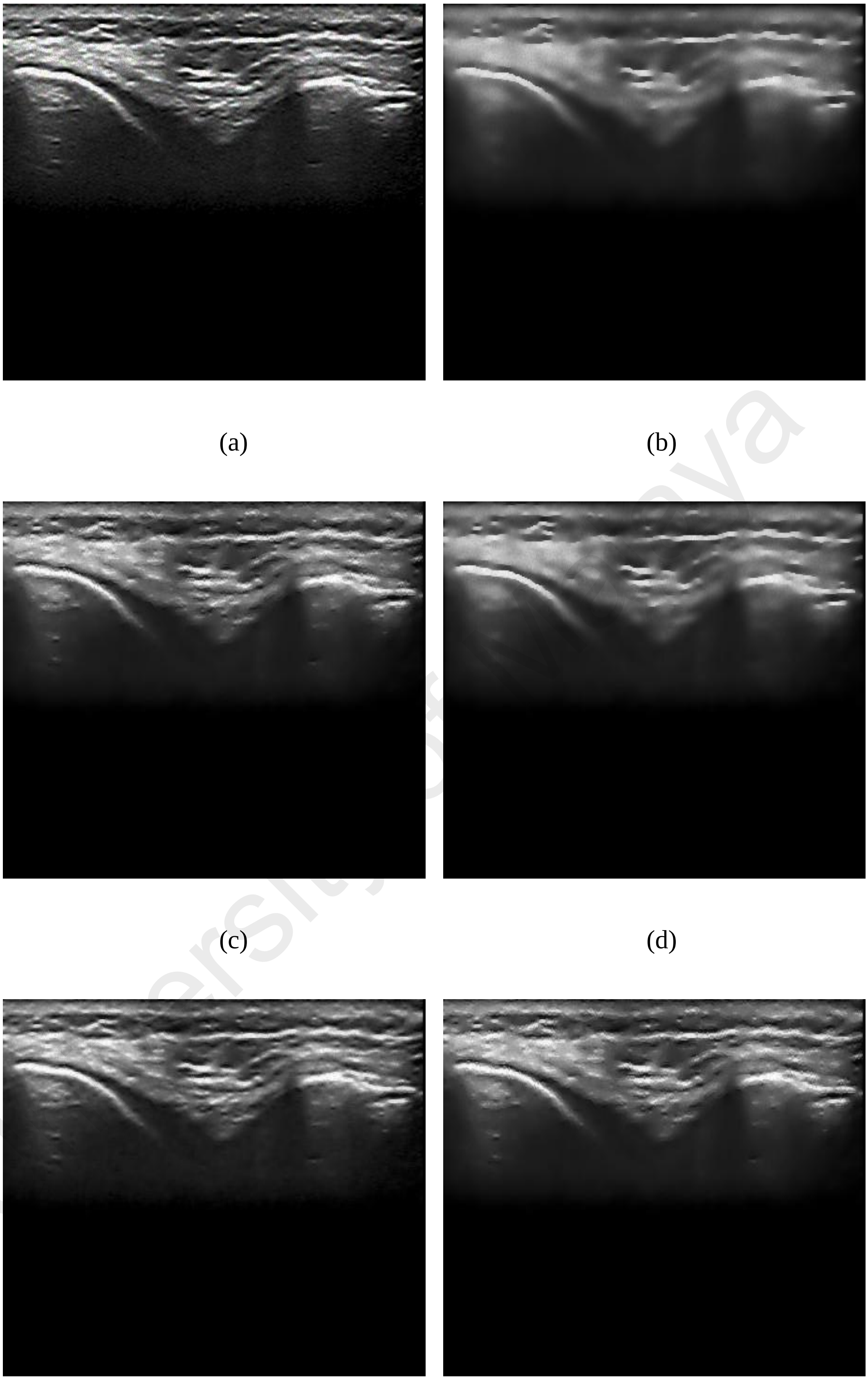

Figure 4.8: Fifth example of US image of knee joint cartilage (a) Original Image. AD filtered images by using (b) PM method (c) LPND (d) NCD (e) SRAD (f) OSRAD

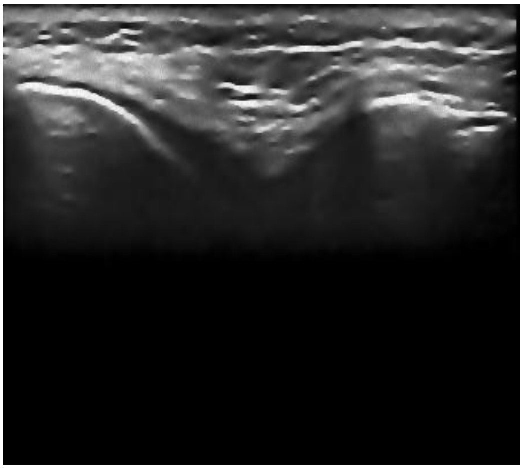

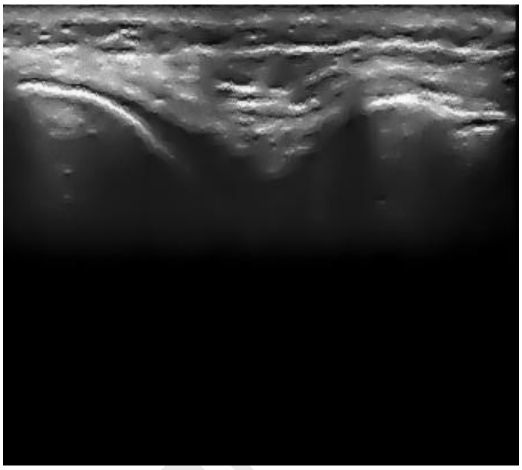

(g) (h)

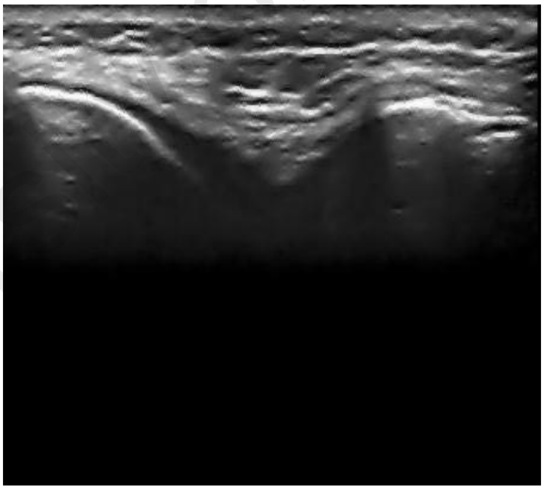

(i)

Figure 4.8, continued: AD filtered images by using (g) DPAD (h) Wavelet (i) proposed Model

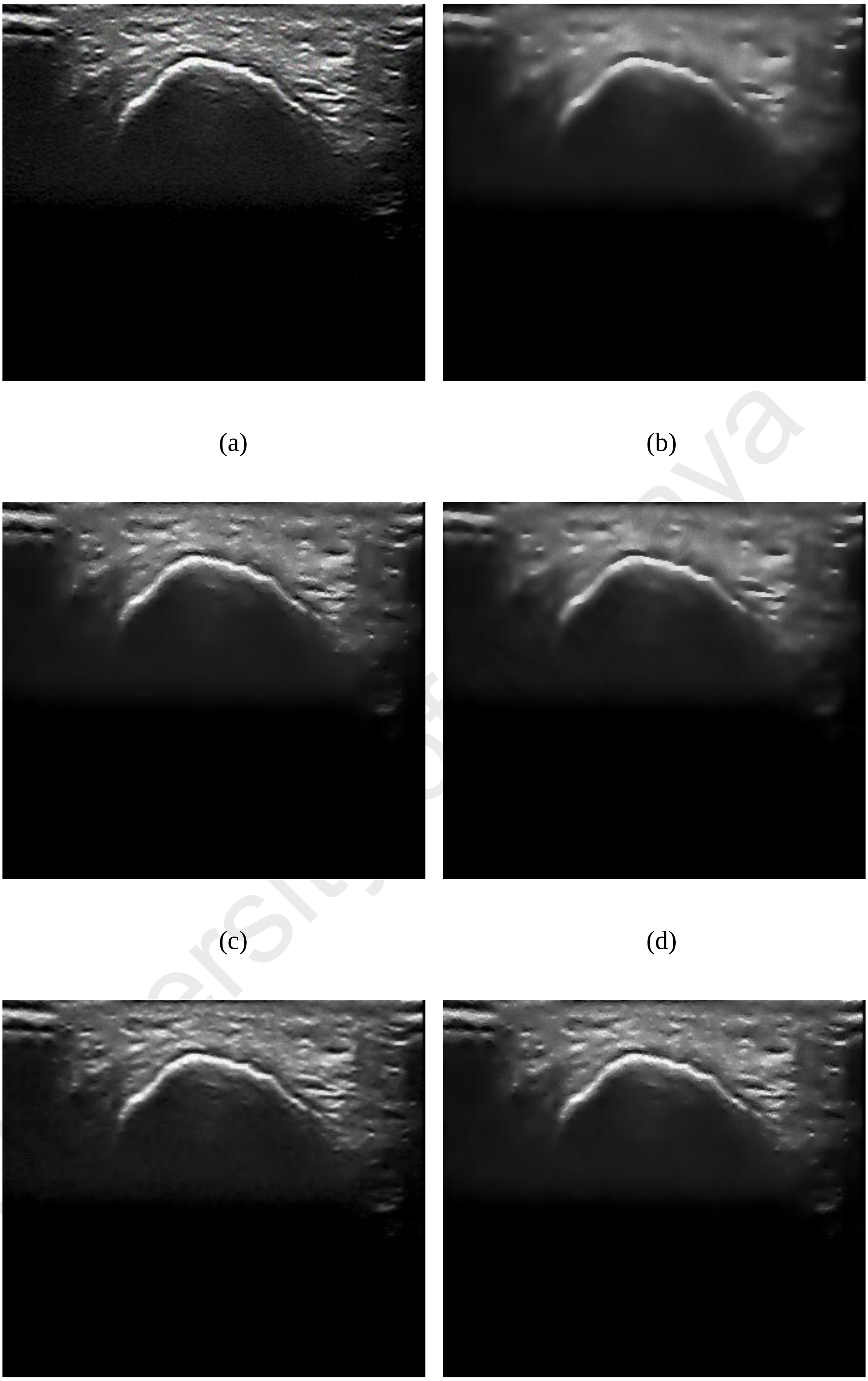

(a) (b)

(c) (d)

(e) (f)

Figure 4.9: Sixth example of US image of knee joint cartilage (a) Original Image. AD filtered images by using (b) PM model (c) LPND (d) NCD (e)SRAD (f) OSRAD

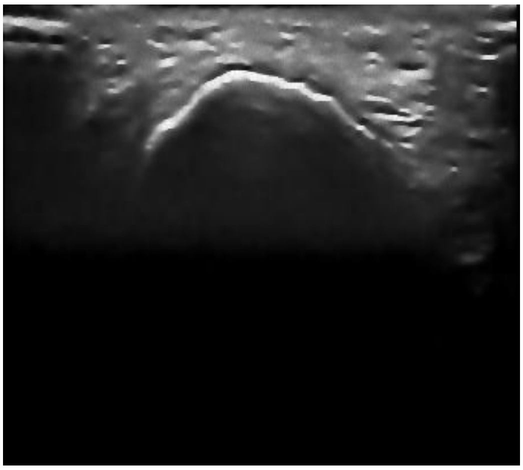

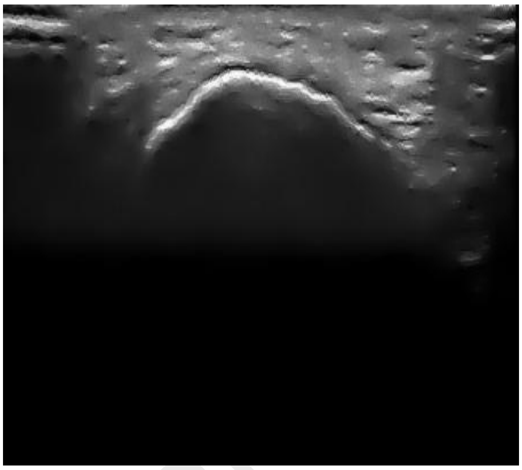

(g) (h)

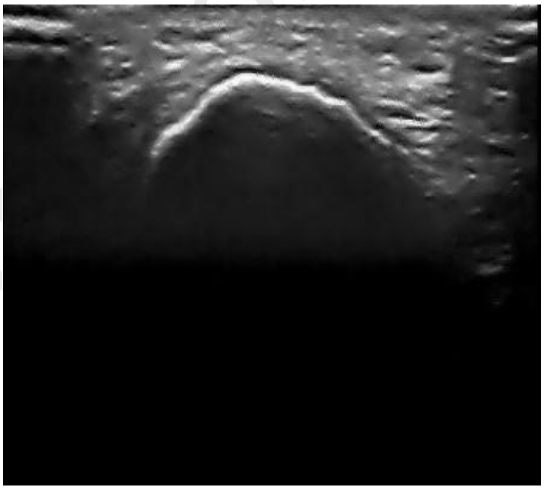

(i)

Figure 4.9, continued: AD filtered images by using (g) DPAD (h) Wavelet (i) proposed Model

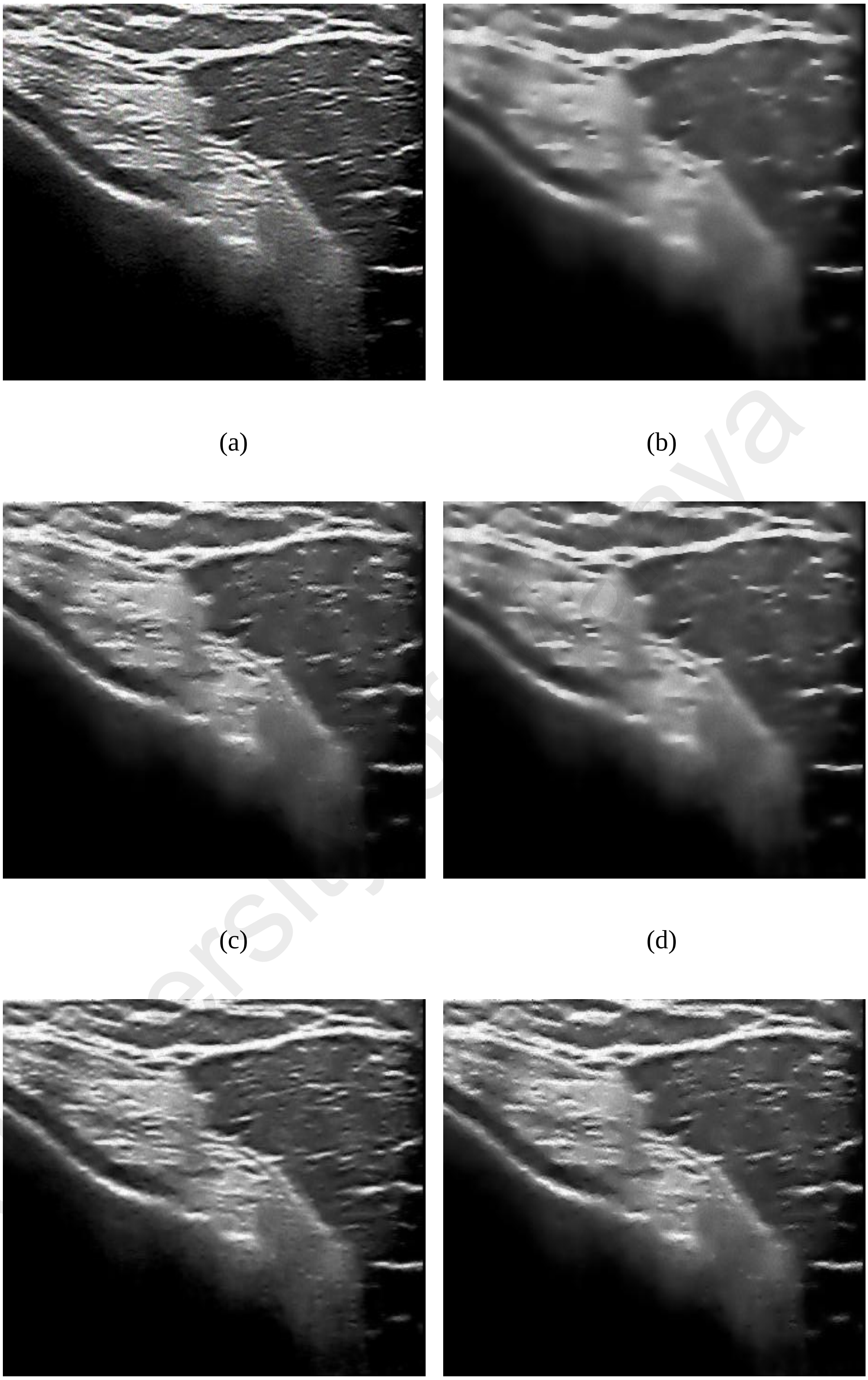

(a) (b)

(c) (d)

(e) (f)

Figure 4.10: Seventh example of US image of knee joint cartilage (a) Original Image. AD filtered images by using (b) PM model (c) LPND (d) NCD (e) SRAD (f) OSRAD

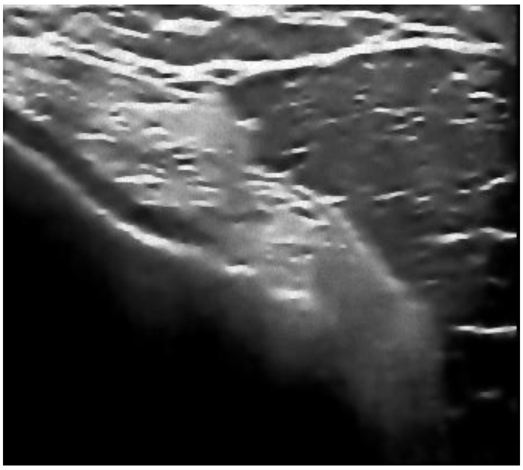 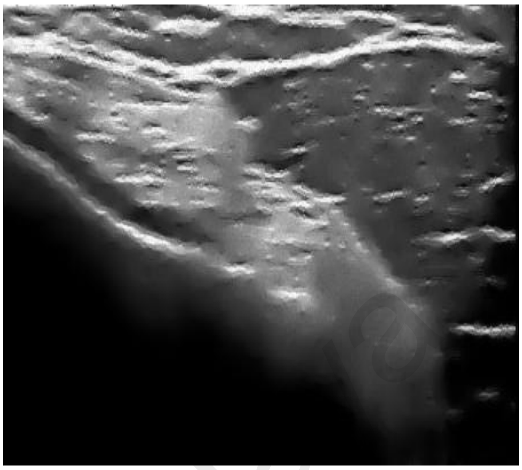

(g) (h)

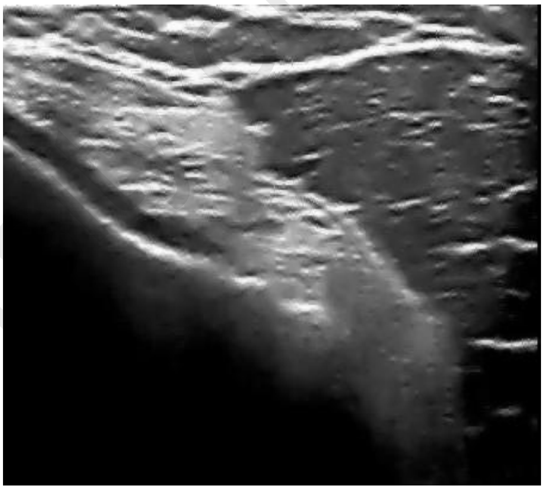

(i)

Figure 4.10, continued: AD filtered images by using (g) DPAD (h) Wavelet (i) proposed Model

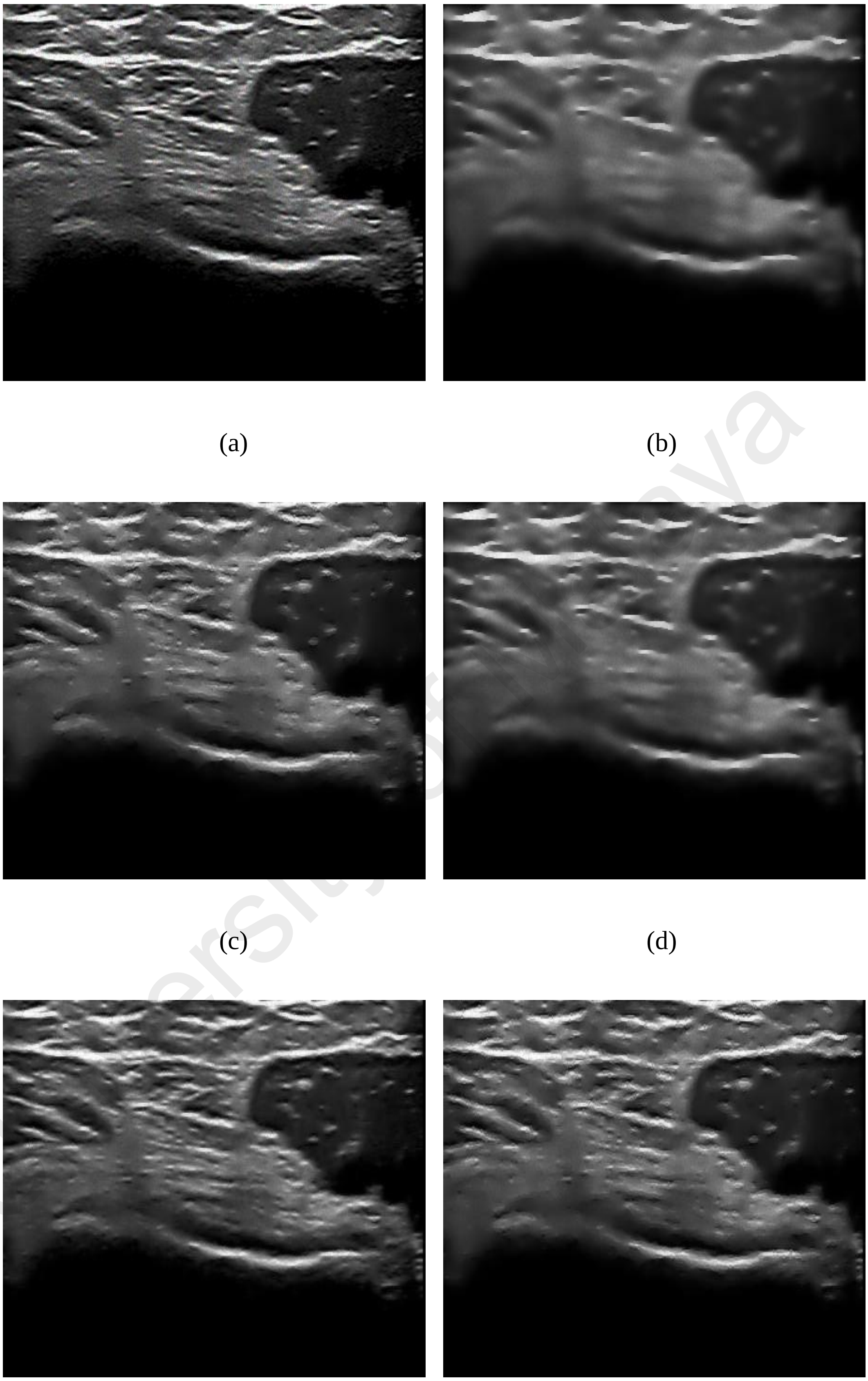

Figure 4.11: Eight example of the US image of knee joint cartilage (a) Original Image. AD filtered images by using (b) PM model (c) LPND (d) NCD (e) SRAD (f) OSRAD

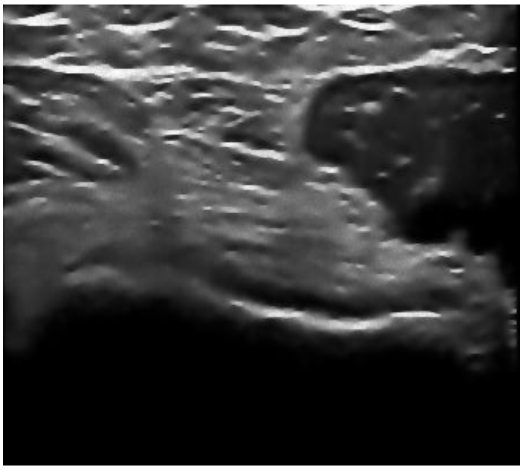

(g)

(h)

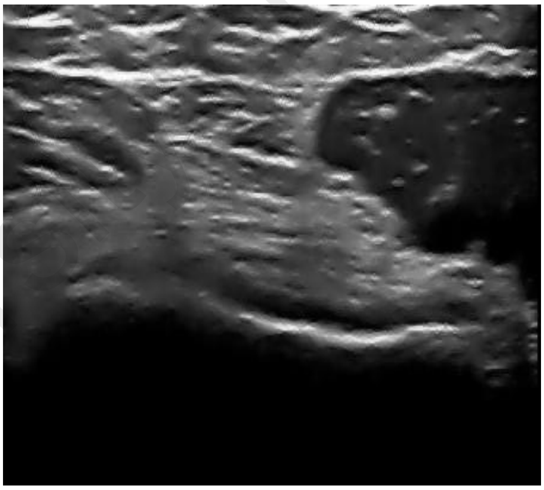

(i)

Figure 4.11, continued: AD filtered images by using (g) DPAD (h) Wavelet (i) proposed Model

4.5 Quantitative Analysis

For quantitative analysis, four different matrices PSNR, SSIM, FOM, and ENL are used as described in Section 3.7 First, the results of the proposed model are presented and then the comparison of the proposed model with other methods is also described.

4.5.1 Results of Proposed Model

The performance of the proposed model is evaluated using all thirty images of healthy volunteers. The PSNR values of all data are shown in Figure 4.12. The highest value attain is 33.814 and the lowest value of PSNR using proposed model is 32.989. None of other method have even highest value in this range. This depicts that proposed technique raise the PSNR very well by removing the speckle noise.

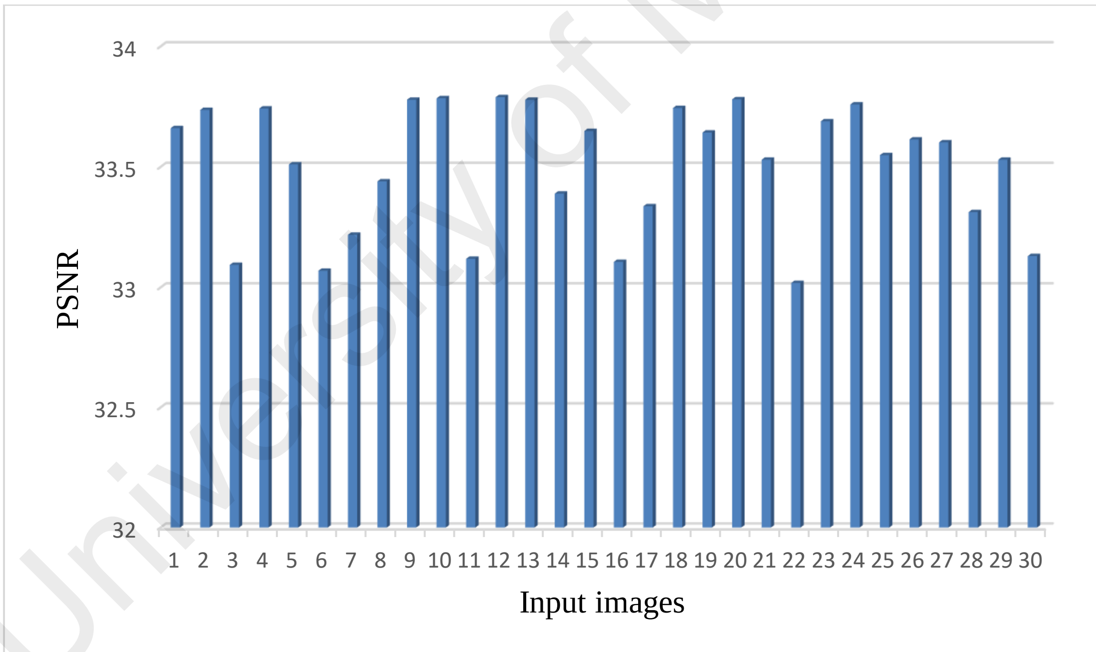

Figure 4.12: PSNR values of all thirty images using the proposed model

SSIM values of thirty images are presented in Figure 4.13. The model has very good values for SSIM. The values range from 0.860 to 0.896 which infers that perceptual quality of image is also enhanced.

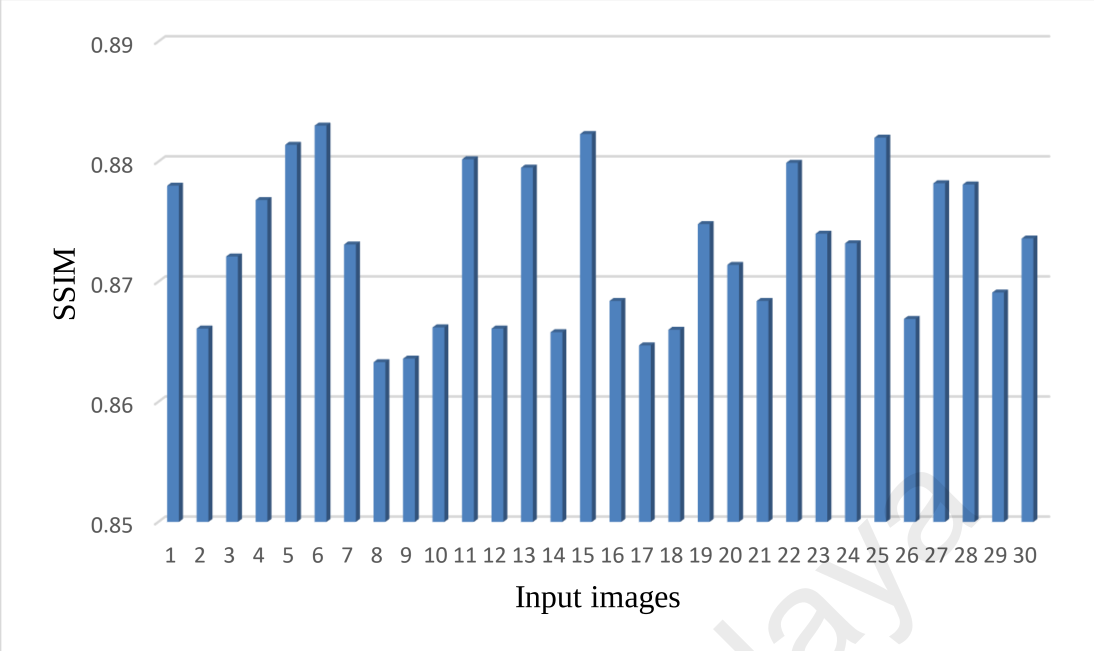

Figure 4.13: SSIM Values of thirty images using the proposed model

The edge detection ability of the model is measured using the FOM. The minimum value of FOM attain is 0.731 and a maximum of 0.811 as presented in Figure 4.14. The FOM values of all images are in very good range which shows that proposed method has the very good ability to preserve the edges.

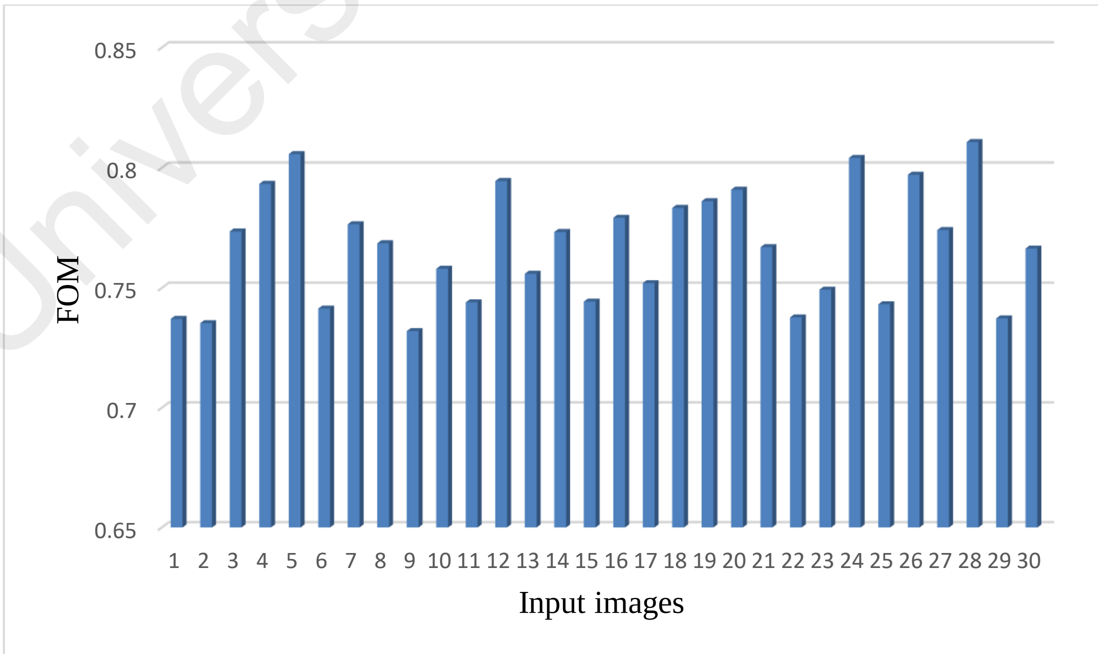

Figure 4.14: FOM values of thirty images using the proposed model

Speckle noise reduction of the proposed model is measured by ENL. Figure 4.15 shows the ENL values of all thirty images using the proposed model. The lowest value of ENL attain is 30.654 and this is higher than ENL value of any other model. This also enforce the argument that proposed model removes the noise efficiently.

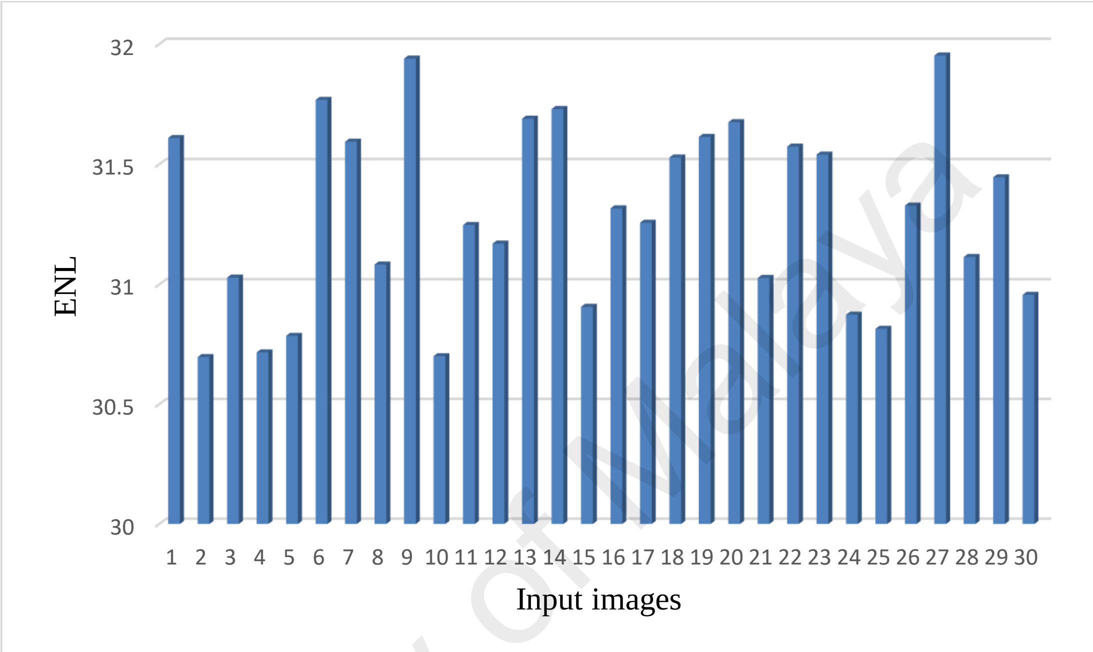

Figure 4.15: ENL values of thirty images using the proposed model

4.5.2 Quantitative Comparison of Proposed Model with other Methods

Using the same four quantitative metrics, PSNR, SSIM, FOM, and ENL, performance comparison of the proposed model with eight other models is evaluated. PM model, SRAD, NCD, OSRAD, DPAD, LPND, wavelet-based, and fuzzy logic-based models are analyzed and compared with the proposed method. All thirty images are used for the analysis.

First, the mean square error of all thirty images is calculated. From MSE the PSNR of all data is measured. Figure 4.16 shows the mean values of PSNR of all different methods. It is depicted from the figure that the proposed methods reduce the noise better compare to all other techniques. This infers that the proposed model is better in removing the speckle noise.

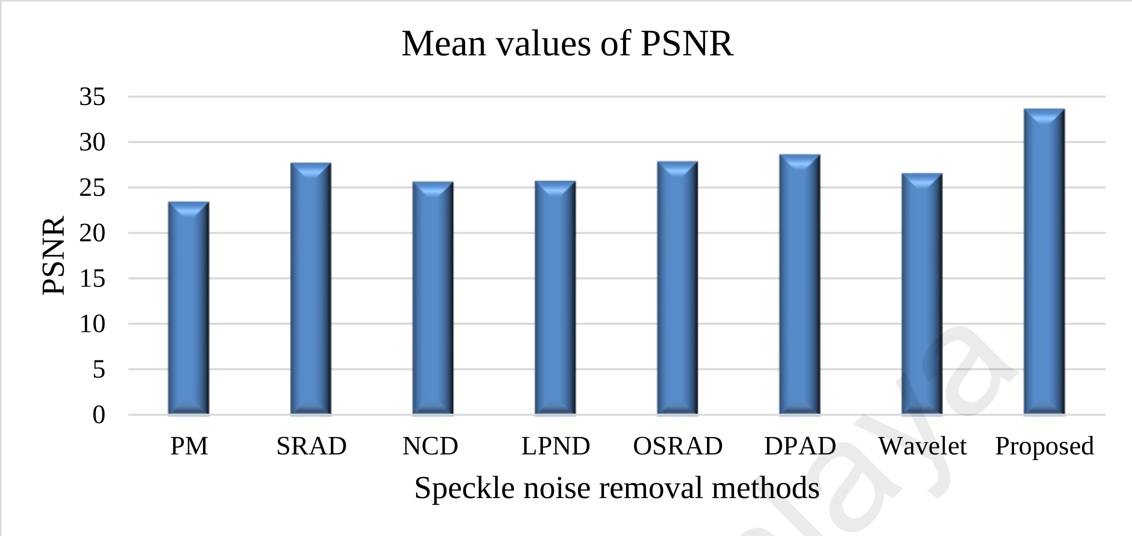

Figure 4.16: PSNR values of the proposed model and PM model

Figure 4.17 shows the mean values of FOM of eight different models and the proposed methods. The FOM measures the ability of edges preservations. The graphs clearly show that the proposed method preserves the edges efficiently.

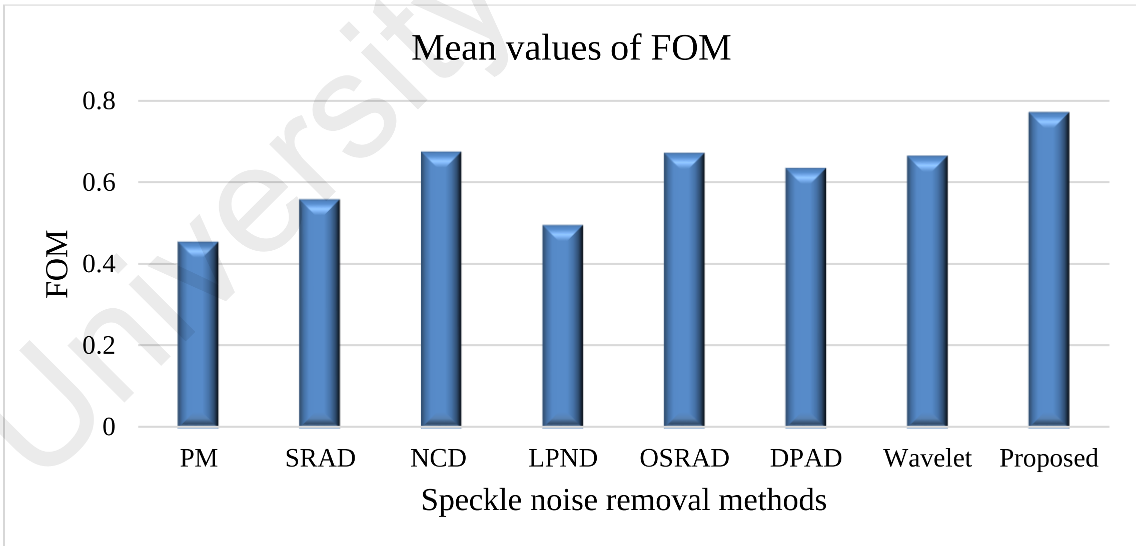

Figure 4.17: FOM values of proposed model and PM model

SSIM is a perceptual measure of human capability. Figure 4.18 is the mean values of SSIM of all methods. The mean SSIM value of the proposed model is 0.873, which is the best value among all others. Although the SSIM value of SRAD is close enough to the proposed model but we can compare the overall performance of the proposed technique by comparing the results of other evaluation metrices. The PSNR and FOM values of proposed model are much better than SRAD, this describes the better performance of proposed model.

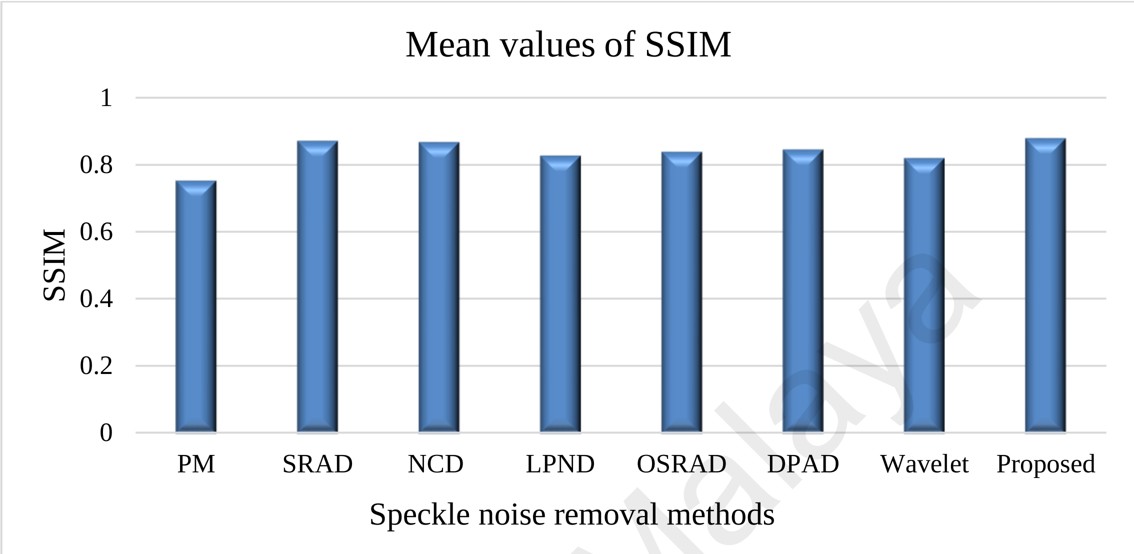

Figure 4.18: SSIM values of proposed Model and PM model

Similarly, the comparison of mean ENL values of proposed and other eight models is shown in Figure 4.19. It is also shown that the proposed model performs better in terms of noise removal. The performance of proposed model and ENL very similar but PSNR values of these two models illustrate that overall noise removal ability of proposed model is better than SRAD.

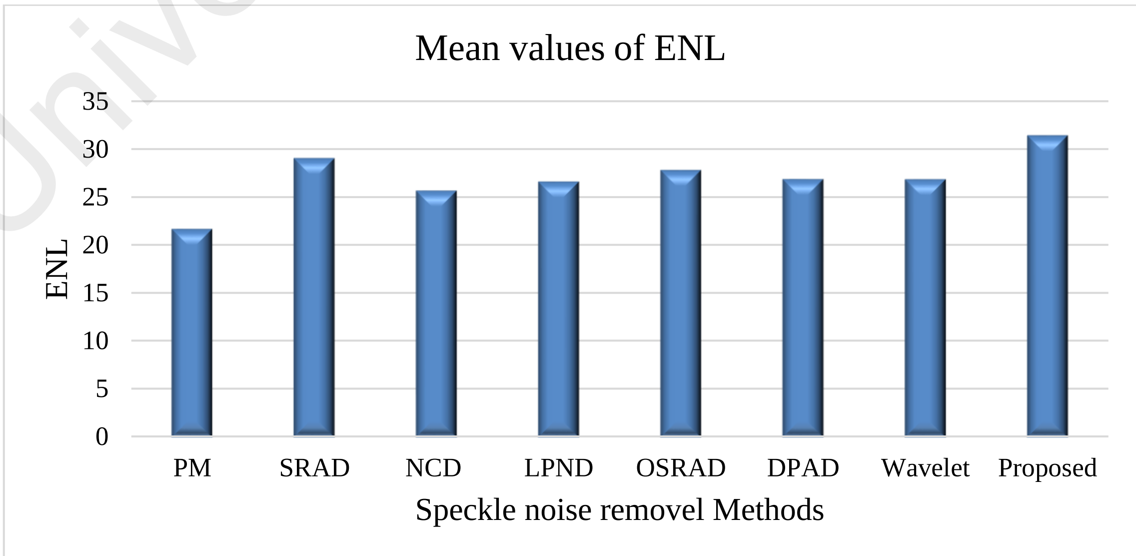

Figure 4.19: ENL values of proposed model and PM model

Table 4.1 shows all the statistics of four evaluation metrics. The 30 ultrasound images are filtered to remove speckle noise using seven different methods and the proposed technique. The evaluations matrices are applied on all thirty images and the output values are stored. The minimum and maximum of PSNR, SSIM, FOM, and ENL from thirty images are mentioned in the table. To evaluate the noise reduction ability of the models, PSNR and ENL matrices are used. The proposed model has a value of 33.503 and 31.290 for PSNR and ENL respectively. These are the highest values among all other methods which depict that the proposed model has removed the speckle noise very well and its performance is finest among all other methods. Similarly, the SSIM value of the proposed method infers that the perceptual visualization of the output image by the proposed model is very good. Furthermore, edge preservation ability is analyzed by FOM. The proposed model attains the highest value 0.873 value for FOM. It confirms that the proposed method also preserves the edges efficiently. So, the mean and standard deviation show that the proposed method outperforms the other models not only in terms of noise reduction but also in edge preservation.

Table 4.1: Mean value for PSNR, SSIM, FOM, and ENL with standard deviations.

Evaluation Metric →	PSNR			SSIM			FOM			ENL		
Method ↓	**Mean ±SD**	**Lower Limit**	**Upper Limit**	**Mean ±SD**	**Lower Limit**	**Upper Limit**	**Mean ±SD**	**Lower Limit**	**Upper Limit**	**Mean ±SD**	**Lower Limit**	**Upper Limit**
PM	23.300± 0.976	22.410	24.029	0.747± 0.054	0.699	0.787	0.450± 0.041	0.401	0.480	21.501± 0.612	20.189	22.345
LPND	25.576± 0.609	24.981	26.123	0.822± 0.027	0.797	0.850	0.491± 0.023	0.459	0.512	26.451 ± 0.761	24.991	27.309
NCD	25.502± 0.810	24.543	25.994	0.862± 0.017	0.820	0.889	0.671± 0.031	0.529	0.591	25.512± 0.490	24.346	26.231
SRAD	27.598± 0.581	26.891	28.276	0.866± 0.014	0.839	0.891	0.554± 0.013	0.536	0.581	28.910± 0.308	27.981	29.222
OSRAD	27.715± 0.395	27.019	28.298	0.833± 0.015	0.802	0.859	0.668± 0.010	0.654	0.680	27.651± 0.771	26.815	28.107
DPAD	28.510± 1.105	27.149	29.831	0.840± 0.028	0.815	0.855	0.631± 0.033	0.593	0.667	26.721± 0.892	25.123	27.709
Wavelet	26.407± 0.347	25.946	27.154	0.814± 0.022	0.821	0.852	0.661± 0.019	0.687	0.734	26.710± 0.761	26.221	27.410
Proposed	33.503± 0.2592	32.989	33.814	0.873± 0.0063	0.860	0.896	0.767± 0.0239	0.731	0.811	31.290± 0.384	30.654	32.007

4.6 Summary

In this chapter, the efficiency of the proposed model is presented. The comparison of the proposed and previously used diffusivity function is assessed using simulated images. Edge preservation of the model using one, two, and four gradient thresholds is measured using seismic images which depicts that four gradient thresholds better preserves the edges. The performance of the overall model is compared with the eighth other models using four different metrics. From the qualitative and quantitative results, it can be concluded that the proposed filtering method performs outstandingly in reducing the speckle noise in US images of knee articular cartilage.

CHAPTER 5: CONCLUSION AND FUTURE WORK

In this study, a despeckling method based on AD for the knee US images is proposed. All steps of AD methods are studied and proposed a robust and efficient algorithm to remove the speckle noise. The proposed new algorithm is coded in MATLAB R2018a software.

The database of knee US images of thirty healthy volunteers is collected for this research. Images are passed through the Gaussian filter to remove the additive gaussian noise. This is done to ensure that Gaussian noise is removed before the calculation of the image gradient as the diffusion in the AD method is based on the gradient value of the image. The performance of the method is enhanced by calculating the gradient in eight neighborhood directions. Unlike the previous studies which use one or two thresholds, here four gradient thresholds are measured in NS, EW, NWES and NSWE directions. Thresholds in four different directions provide more flexibility in the diffusion process and image is diffused differently in each direction depending upon the threshold value. These thresholds are calculated using a knee algorithm using these eight gradients.

While removing the noise diffusion rate and to stop the diffusion across the boundaries in the image are the main tasks. These tasks are performed by a diffusivity function. A diffusivity function is proposed which not only performs diffusion but also preserves the edges efficiently. Diffusivity functions are the functions of threshold values so using four thresholds, four different values of diffusivity functions are obtained. These four values diffusivity functions perform and stop the diffusion differently in each direction.

The diffusion process is an iterative process that is to be performed several times to remove the speckle noise and get the desired speckle free image. The number of iterations depends upon the noise level and image type. Therefore, using the fixed number of iterations cannot give better results and are not robust. To automatically stop the diffusion, MAE is used. After each iteration, the MAE value of the image is calculated and is compared with the predefined threshold. If the value of MAE is larger than the threshold, the diffusion process is continued while diffusion is stopped when MAE is less than a threshold. In this way the diffusion is automatically is stopped and hence makes the process more robust.

The performance of the proposed method is evaluated using both quantitative and qualitative analyses. The performance of the proposed diffusivity function is analyzed using the simulated images while the effect of using four gradient thresholds is shown by seismic images. The overall performance of the proposed method is evaluated using knee US images. Four different evaluation metrics PSNR, SSIM, FOM, and ENL are used. Numerical results depict that proposed methods perform better not only in noise removal but also in edge preservation.

In the future, research work will be focused on the processing time of the proposed model. Although the method performs very well by calculating four gradients and performing different diffusion in each different direction, but this process takes more time as compared to other methods. If the gradient is very low in any direction, the calculation of the gradient threshold and diffusivity in that direction can be skipped. This approach can save time by not calculating and performing diffusivity in that direction. Research can be done to find out the appropriate low value of gradient, based on some theoretical ground to exempt the process in that particular direction.

REFERENCES

Aja-Fernandez, S., & Alberola-Lopez, C. (2006). On the estimation of the coefficient of variation for anisotropic diffusion speckle filtering. *IEEE Transactions on Image Processing*, *15*(9), 2694–2701. https://doi.org/10.1109/TIP.2006.877360

Amirmazlaghani, M., & Amindavar, H. (2012). Wavelet domain Bayesian processor for speckle removal in medical ultrasound images. *IET Image Processing*, *6*(5), 580–588. https://doi.org/10.1049/iet-ipr.2009.0110

Black, M. J., Sapiro, G., Marimont, D. H., & Heeger, D. (1998). Robust anisotropic diffusion. *IEEE Transactions on Image Processing*, *7*(3), 421–432. https://doi.org/10.1109/83.661192

Catté, F., Lions, P.-L., Morel, J.-M., & Coll, T. (1992). Image Selective Smoothing and Edge Detection by Nonlinear Diffusion. *SIAM Journal on Numerical Analysis*, *29*(1), 182–193. https://doi.org/10.1137/0729012

Chen, Y., Yin, R., Flynn, P., & Broschat, S. (2003). Aggressive region growing for speckle reduction in ultrasound images. *Pattern Recognition Letters*, *24*(4–5), 677–691. https://doi.org/10.1016/S0167-8655(02)00174-5

Choi, H., & Jeong, J. (2018). Speckle noise reduction in ultrasound images using SRAD and guided filter. *2018 International Workshop on Advanced Image Technology, IWAIT 2018*, 1–4. https://doi.org/10.1109/IWAIT.2018.8369653

Czerwinski, R. N., Jones, D. L., & O'Brien, W. D. (1999). Detection of lines and boundaries in speckle images - application to medical ultrasound. *IEEE Transactions on Medical Imaging*, *18*(2), 126–136. https://doi.org/10.1109/42.759114

Dutt, V., & Greenleaf, J. F. (1996). Adaptive speckle reduction filter for log-compressed B-scan images. *IEEE Transactions on Medical Imaging*, *15*(6), 802–813. https://doi.org/10.1109/42.544498

Faisal, A., Ng, S. C., Goh, S. L., George, J., Supriyanto, E., & Lai, K. W. (2015). Multiple LREK Active Contours for Knee Meniscus Ultrasound Image Segmentation. *IEEE Transactions on Medical Imaging*, *34*(10), 2162–2171. https://doi.org/10.1109/TMI.2015.2425144

Frost, V. S., Stiles, J. A., Shanmugan, K. S., & Holtzman, J. C. (1982). A Model for Radar Images and Its Application to Adaptive Digital Filtering of Multiplicative Noise. *IEEE Transactions on Pattern Analysis and Machine Intelligence*, *PAMI-4*(2), 157–166. https://doi.org/10.1109/TPAMI.1982.4767223

Gagnon, L., & Jouan, A. (2004). Speckle filtering of SAR images: a comparative study between complex-wavelet-based and standard filters. *Wavelet Applications in Signal and Image Processing V*, *3169*, 80–91. https://doi.org/10.1117/12.279681

Gohal, C., Shanmugaraj, A., Tate, P., Horner, N. S., Bedi, A., Adili, A., & Khan, M. (2018). Effectiveness of Valgus Offloading Knee Braces in the Treatment of Medial

Compartment Knee Osteoarthritis: A Systematic Review. *Sports Health*, *10*(6), 500–514. https://doi.org/10.1177/1941738118763913

Guo, F., Zhang, G., Zhang, Q., Zhao, R., Deng, M., & Xu, K. (2018). Speckle suppression by weighted euclidean distance anisotropic diffusion. *Remote Sensing*, *10*(5), 1–20. https://doi.org/10.3390/rs10050722

Guo, L., Xu, Y., Xu, Z., & Jiang, J. (2015). A PDE-based regularization algorithm toward reducing speckle tracking noise: A feasibility study for ultrasound breast elastography. *Ultrasonic Imaging*, *37*(4), 277–293. https://doi.org/10.1177/0161734614561128

Guy, G., Nir, S., & Yehoshua Y., Z. (2004). Image Enhancement and Denoising by Complex Diffusion Processes. *IEEE Transactions on Pattern Analysis and Machine Intelligence*, *26*(8), 1020–1036.

Hossain, M. B., Lai, K. W., Pingguan-Murphy, B., Hum, Y. C., Mohd Salim, M. I., & Liew, Y. M. (2014). Contrast enhancement of ultrasound imaging of the knee joint cartilage for early detection of knee osteoarthritis. *Biomedical Signal Processing and Control*, *13*(1), 157–167. https://doi.org/10.1016/j.bspc.2014.04.008

Hou, J., Lv, X., & Chen, Q. (2019). Research on ultrasonic image processing algorithm based on anisotropic diffusion. *Journal of Computational Methods in Sciences and Engineering*, *19*(S1), S325–S329. https://doi.org/10.3233/JCM-191047

Huang, H. C., Chen, J. Y., Wang, S. De, & Chen, C. M. (2003). Adaptive ultrasonic speckle reduction based on the slope-facet model. *Ultrasound in Medicine and Biology*, *29*(8), 1161–1175. https://doi.org/10.1016/S0301-5629(03)00927-X

Hummel, R. A. (1987). Representations based on Zero-crossings in Scale-Space. In *Readings in Computer Vision* (pp. 753–758). Elsevier. https://doi.org/10.1016/B978-0-08-051581-6.50072-6

Jain, S. K., Ray, R. K., & Bhavsar, A. (2019). A Nonlinear Coupled Diffusion System for Image Despeckling and Application to Ultrasound Images. *Circuits, Systems, and Signal Processing*, *38*(4), 1654–1683. https://doi.org/10.1007/s00034-018-0913-6

Joel, T., & Sivakumar, R. (2018). An extensive review on Despeckling of medical ultrasound images using various transformation techniques. *Applied Acoustics*, *138*(February), 18–27. https://doi.org/10.1016/j.apacoust.2018.03.023

Kamalaveni, V., Rajalakshmi, R. A., & Narayanankutty, K. A. (2015). Image Denoising Using Variations of Perona-Malik Model with Different Edge Stopping Functions. *Procedia Computer Science*, *58*, 673–682. https://doi.org/10.1016/j.procs.2015.08.087

Karaman, M., Karaman, M., Kutay, M. A., & Bozdagi, G. (1995). An Adaptive Speckle Suppression Filter for Medical Ultrasonic Imaging. *IEEE Transactions on Medical Imaging*, *14*(2), 283–292. https://doi.org/10.1109/42.387710

Ker, J., Wang, L., Rao, J., & Lim, T. (2017). Deep Learning Applications in Medical Image Analysis. *IEEE Access*, *6*, 9375–9379.

https://doi.org/10.1109/ACCESS.2017.2788044

Krissian, K., Westin, C.-F., Kikinis, R., & Vosburgh, K. G. (2007). Oriented Speckle Reducing Anisotropic Diffusion. *IEEE Transactions on Image Processing*, *16*(5), 1412–1424. https://doi.org/10.1109/TIP.2007.891803

Kuan, D., Sawchuk, A., Strand, T., & Chavel, P. (1987). Adaptive restoration of images with speckle. *IEEE Transactions on Acoustics, Speech, and Signal Processing*, *35*(3), 373–383. https://doi.org/10.1109/TASSP.1987.1165131

Kulkarni, P., & Madathil, D. (2019). Adaptive Thresholding Method for Speckle Reduction of Echocardiographic Images. *IETE Journal of Research*, *0*(0), 1–9. https://doi.org/10.1080/03772063.2019.1634494

Kunz, D., Eck, K., Fillbrandt, H., & Aach, T. (2003). Nonlinear multiresolution gradient adaptive filter for medical images. In M. Sonka & J. M. Fitzpatrick (Eds.) (p. 732). https://doi.org/10.1117/12.481323

Lattari, F., Leon, B. G., Asaro, F., Rucci, A., Prati, C., & Matteucci, M. (2019). Deep learning for SAR image despeckling. *Remote Sensing*, *11*(13), 1–20. https://doi.org/10.3390/rs11131532

Lee, J.-S., Grunes, M. R., & Mango, S. A. (1991). Speckle reduction in multipolarization, multifrequency SAR imagery. *IEEE Transactions on Geoscience and Remote Sensing*, *29*(4), 535–544. https://doi.org/10.1109/36.135815

Li, X., & Chen, T. (1994). Nonlinear diffusion with multiple edginess thresholds. *Pattern Recognition*, *27*(8), 1029–1037. https://doi.org/10.1016/0031-3203(94)90142-2

Ling, H., & Bovik, A. C. (2002). Smoothing low-SNR molecular images via anisotropic median-diffusion. *IEEE Transactions on Medical Imaging*, *21*(4), 377–384. https://doi.org/10.1109/TMI.2002.1000261

Lopes, A., Nezry, E., Touzi, R., & Laur, H. (1993). Structure detection and statistical adaptive speckle filtering in SAR images. *International Journal of Remote Sensing*, *14*(9), 1735–1758. https://doi.org/10.1080/01431169308953999

Lopes, Armand, Touzi, R., & Nezry, E. (1990). Adaptive Speckle Filters and Scene Heterogeneity. *IEEE Transactions on Geoscience and Remote Sensing*, *28*(6), 992–1000. https://doi.org/10.1109/36.62623

Loupas, T., McDicken, W. N., & Allan, P. L. (1989). An adaptive weighted median filter for speckle suppression in medical ultrasonic images. *IEEE Transactions on Circuits and Systems*, *36*(1), 129–135. https://doi.org/10.1109/31.16577

Ma, X., Shen, H., Zhang, L., Yang, J., & Zhang, H. (2015). Adaptive Anisotropic Diffusion Method for Polarimetric SAR Speckle Filtering. *IEEE Journal of Selected Topics in Applied Earth Observations and Remote Sensing*, *8*(3), 1041–1050. https://doi.org/10.1109/JSTARS.2014.2328332

Mandal, J. K., Satapathy, S. C., Sanyal, M. K., & Bhateja, V. (2017). Preface. *Advances in Intelligent Systems and Computing*, *458*, v–vi. https://doi.org/10.1007/978-981-

10-2035-3

Nageswari, P., Rajan, S., & Manivel, K. (2017). A comparative study of despeckling filters for enhancement of medical images. *2017 Conference on Emerging Devices and Smart Systems, ICEDSS 2017*, (March), 155–160. https://doi.org/10.1109/ICEDSS.2017.8073676

Penna, P. A. A., & Mascarenhas, N. D. A. (2019). SAR Speckle Nonlocal Filtering With Statistical Modeling of Haar Wavelet Coefficients and Stochastic Distances. *IEEE Transactions on Geoscience and Remote Sensing*, *57*(9), 7194–7208. https://doi.org/10.1109/tgrs.2019.2912153

Perona, P., & Malik, J. (1990). Scale-space and edge detection using anisotropic diffusion. *IEEE Transactions on Pattern Analysis and Machine Intelligence*, *12*(7), 629–639. https://doi.org/10.1109/34.56205

Petrou, M., & Petrou, C. (2010). *Image Processing: The Fundamentals www.it-ebooks.info*. Retrieved from https://the-eye.eu/public/Books/IT Various/Image Processing%2C 2nd Edition.pdf

Terebes, R., Borda, M., Germain, C., Malutan, R., & Ilea, I. (2016). A multiplicative gradient-based anisotropic diffusion approach for speckle noise removal. *2015 E-Health and Bioengineering Conference, EHB 2015*, (3). https://doi.org/10.1109/EHB.2015.7391605

Tsiotsios, C., & Petrou, M. (2013). On the choice of the parameters for anisotropic diffusion in image processing. *Pattern Recognition*, *46*(5), 1369–1381. https://doi.org/10.1016/j.patcog.2012.11.012

Tur, M., Chin, K. C., & Goodman, J. W. (1982). When is speckle noise multiplicative? *Applied Optics*, *21*(7), 1157. https://doi.org/10.1364/ao.21.001157

University of tartu. (2014). *1. Introduction to image processing | Digital Image Processing*. *January 2014*. Retrieved from https://sisu.ut.ee/imageprocessing/book/1

Wang, B., Chapron, B., Mercier, G., Garello, R., & He, M.-X. (2011). Polarimetric characteristics of ships on RADARSAT-2 data. In *OCEANS 2011 IEEE - Spain* (pp. 1–4). IEEE. https://doi.org/10.1109/Oceans-Spain.2011.6003583

Wang, Z., Bovik, A. C., Sheikh, H. R., & Simoncelli, E. P. (2004). Image Quality Assessment: From Error Visibility to Structural Similarity. *IEEE Transactions on Image Processing*, *13*(4), 600–612. https://doi.org/10.1109/TIP.2003.819861

Wang, Zhou, Simoncelli, E. P., & Bovik, A. C. (2000). Multiscale structural similarity for image quality assessment. In *The Thrity-Seventh Asilomar Conference on Signals, Systems & Computers, 2003* (Vol. 2, pp. 1398–1402). IEEE. https://doi.org/10.1109/ACSSC.2003.1292216

Xu, H., Gong, Y., Xia, X., Li, D., Yan, Z., Shi, J., & Zhang, Q. (2019). Gabor-based anisotropic diffusion with lattice Boltzmann method for medical ultrasound despeckling. *Mathematical Biosciences and Engineering*, *16*(6), 7546–7561.

https://doi.org/10.3934/mbe.2019379

Yongjian Yu, & Acton, S. T. (2002). Speckle reducing anisotropic diffusion. *IEEE Transactions on Image Processing*, *11*(11), 1260–1270. https://doi.org/10.1109/TIP.2002.804276

Yu, H., Ding, M., Zhang, X., & Wu, J. (2018). PCANet based nonlocal means method for speckle noise removal in ultrasound images. *PLoS ONE*, *13*(10), 1–19. https://doi.org/10.1371/journal.pone.0205390

Yu, Jimin, Zhai, R., & Yie, J. (2018). Image denoising method based on PM model with transforming edge stopping function. *Proceedings of the 2017 IEEE 2nd Information Technology, Networking, Electronic and Automation Control Conference, ITNEC 2017*, *2018-Janua*(2), 438–442. https://doi.org/10.1109/ITNEC.2017.8284769

Yu, Jinhua, Tan, J., & Wang, Y. (2010). Ultrasound speckle reduction by a SUSAN-controlled anisotropic diffusion method. *Pattern Recognition*, *43*(9), 3083–3092. https://doi.org/10.1016/J.PATCOG.2010.04.006

Zhang, F., Yoo, Y. M., Koh, L. M., & Kim, Y. (2007). Nonlinear diffusion in laplacian pyramid domain for ultrasonic speckle reduction. *IEEE Transactions on Medical Imaging*, *26*(2), 200–211. https://doi.org/10.1109/TMI.2006.889735

Zhang, K., Zuo, W., Chen, Y., Meng, D., & Zhang, L. (2017). DnCNN. *IEEE Transactions on Image Processing*, *26*(7), 3142–3155. https://doi.org/10.1109/TIP.2017.2662206

Zhou, Z., Guo, Z., Zhang, D., & Wu, B. (2018). A Nonlinear Diffusion Equation-Based Model for Ultrasound Speckle Noise Removal. *Journal of Nonlinear Science*, *28*(2), 443–470. https://doi.org/10.1007/s00332-017-9414-1

LIST OF PUBLICATIONS AND PAPERS PRESENTED

Muhammad Shoaib Ali, Md Belayet Hossain, Yan Chai Hum, Joon Huang Chuah, Maheza Irna Mohd Salim and Khin Wee Lai *, "Speckle Noise Diffusion in Knee Articular Cartilage Ultrasound Images", Current Medical Imaging (2019) 15: 1. https://doi.org/10.2174/1573405615666190903143330

Paper Presented

Name of Article	Conference	Status
Anisotropic Diffusion for Reduction of Speckle-Noise in Knee Articular Cartilage Ultrasound Images	International Conference for Innovation in Biomedical Engineering & Life Sciences (ICIBEL 2019)	Presented